COLUMBIA UNIVERSITY
IN THE CITY OF NEW YORK

Large Cluster Dynamical Mean Field Simulations
Emanuel Gull

A.J. Millis, A. Georges, M. Ferrero, N. Lin, O. Parcollet, P. Werner
S. Fuchs, P. Staar, P. Nukala, M. Summers, T. Pruschke, T. Schulthess, T. Maier
L. Pollet, E. Kozik, E. Burovski, M. Troyer
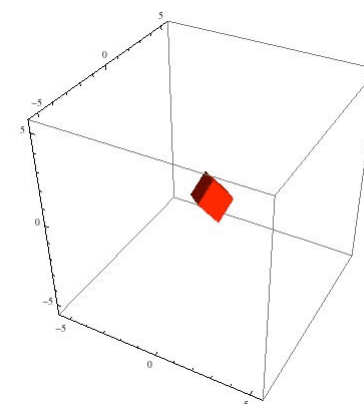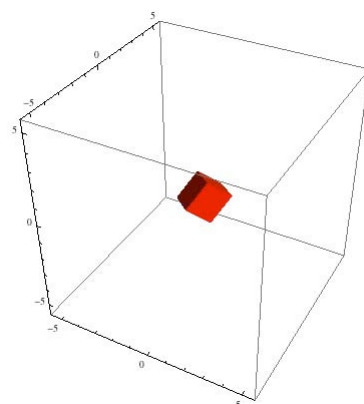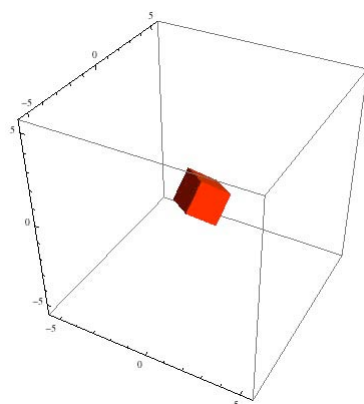KITP, Santa Barbara, Nov. 08 2010

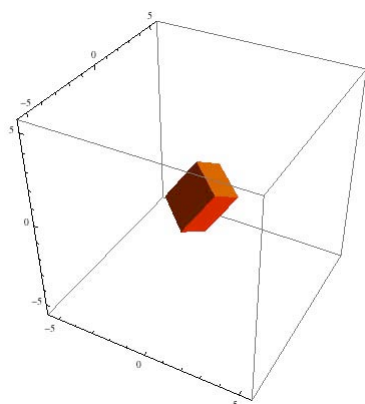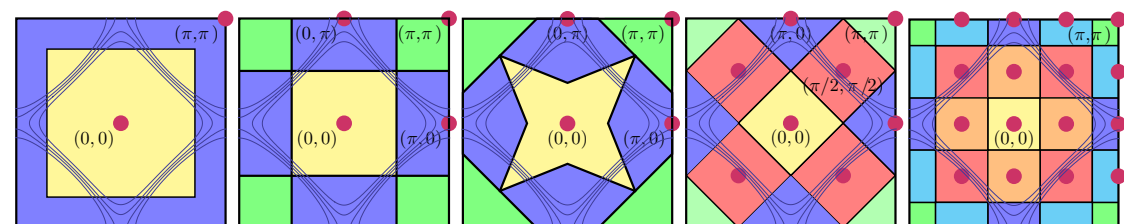Phys. Rev. B 80, 045120 (2009)   Phys. Rev. B 82, 045104 (2010)   arXiv:1009.2759
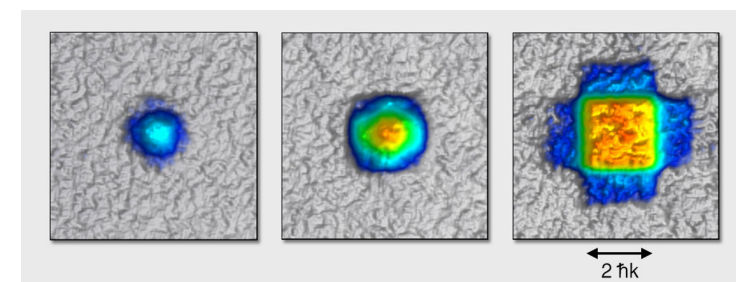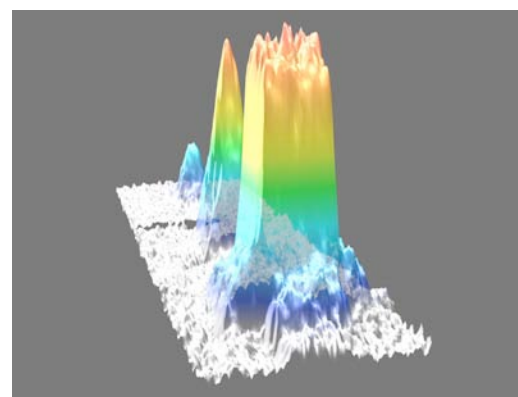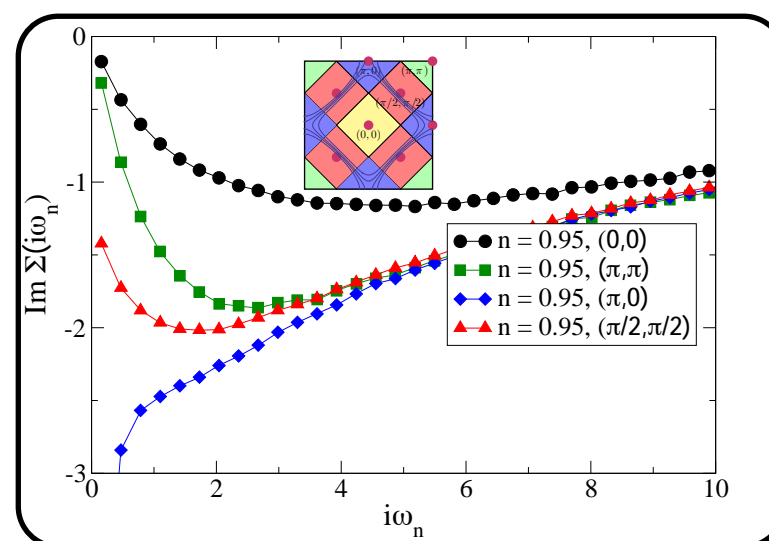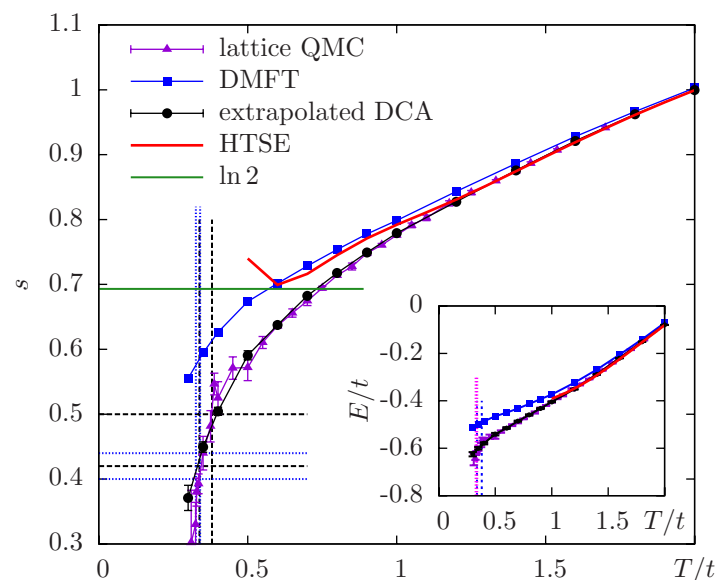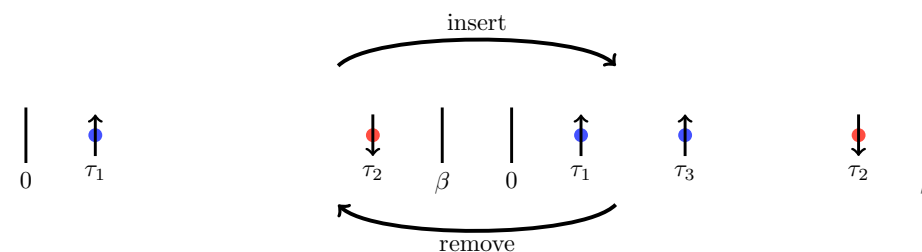Phys. Rev. B 80, 245102 (2009)   Phys. Rev. B 82, 155101 (2010)   arXiv:1010.3690

Overview

Large Cluster Studies – Motivation

Cluster Dynamical Mean Field Theory with large clusters

Impurity solver – Continuous-Time Auxiliary Field with sub-matrix updates

insert

remove

Results – Thermodynamics of the 3D Hubbard model (above T_N), 2D Pseudogap physics

Motivation – Large Cluster Studies

Optical Lattice Systems:
Cold Fermionic Gases

Cold Atomic Gases: goal to simulate
simple model Hamiltonians

T. Esslinger, Annu. Rev. Condens.
Matter Phys. 1, 129-152 (2010)

fermionic case: 3D Hubbard model

$$H = - \sum_{\langle ij \rangle, \sigma} t_{ij} (c_{i\sigma}^\dagger c_{j\sigma} + c_{j\sigma}^\dagger c_{i\sigma}) + U \sum_i n_{i\uparrow} n_{i\downarrow}.$$

Question to theory [numerics]: What is the thermodynamics of this model? (for all fillings, as a function of U/t and T/t? Exact (or controlled) answer is needed.

- Temperatures in experiment are high (for now): When will we reach T_N?

- Qualitative physics is comparatively simple and well understood (no exotic phases, no long range order above T_N)

Motivation – Large Cluster Studies

Controlled answer needed! Need to obtain results (values, error bars) to arbitrary accuracy; no systematic error or uncontrolled approximations.

Candidates:

High Temperature Series Expansion
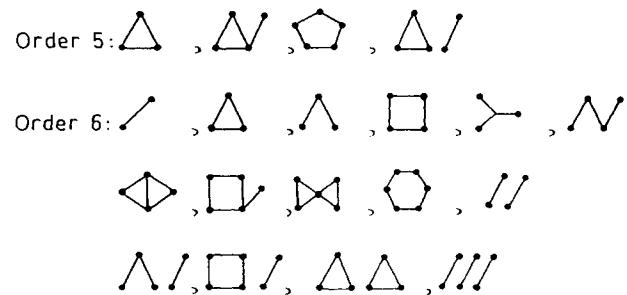
Perfect at high temperature and for nearly empty bands

Henderson et al., Phys. Rev. B 46, 6328 (1992), De Leo et al., arXiv: 1009.2761

Lattice algorithms (BSS, DiagMC, Det. DiagMC)
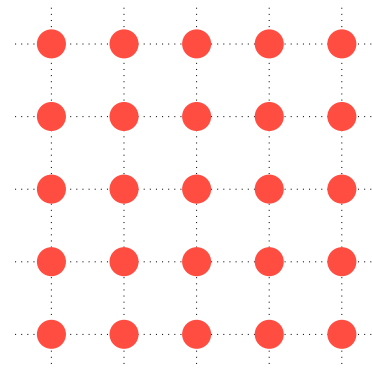
Strong at half filling, bad sign problem away from half filling

Scalettar et al., Phys. Rev. B 39, 4711 (1989), Fuchs et al., arxiv:1009.2759

Single Site **Dynamical Mean Field** Method (+AFM/PM self consistency)

Different philosophy: Single Site DMFT is uncontrolled. (does not necessarily mean bad!)

Motivation – Large Cluster Studies

Another Candidate: Cluster Dynamical Mean Field Theory!

Method based on discretization of the self energy in momentum (or real) space
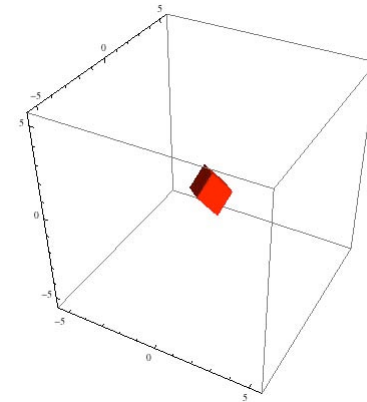
Blocks: patches on which self energy is constant

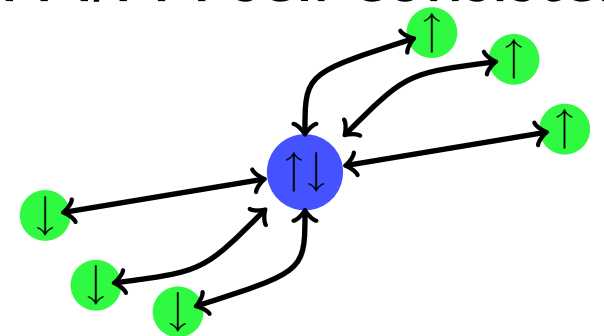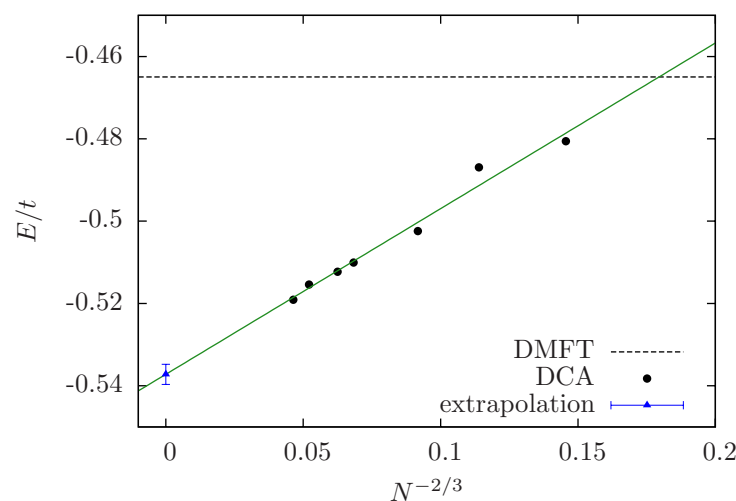Exact limit is obtained by extrapolating to the system with infinite cluster size (as with BSS / DiagMC / other lattice simulations). This needs large enough cluster sizes [here: 48-100 sites]

Why **cluster** DMFT instead of **lattice** methods?

- Convergence is faster than in the lattice simulations.
- Sign problem away from half filling is better in DCA.
- However: Scaling of impurity solver algorithms is worse!

Cluster Dynamical Mean Field Theory

$$\Sigma(k,\omega) = \sum_n \Sigma_n(\omega)\phi_n(k) \approx \sum_n^{N_c} \Sigma_n(\omega)\phi_n(k)$$

Approximation:
Systematic truncation
by cluster sites N_c

$\phi_n(k)$ Basis functions

$\Sigma_n(\omega)$ Energy dependent, k-independent self-energy

'Machinery' for obtaining approximated self energy: Cluster DMFT.

Cluster DMFT is a controlled approximation.

Variants of cluster DMFT: Dynamical Cluster Approximation (used here) and Cellular Dynamical Mean Field Theory: Differ in types of basis functions $\phi_n(k)$

Within DCA: $\phi_n(k)$ chosen to be constant on patches in momentum space.
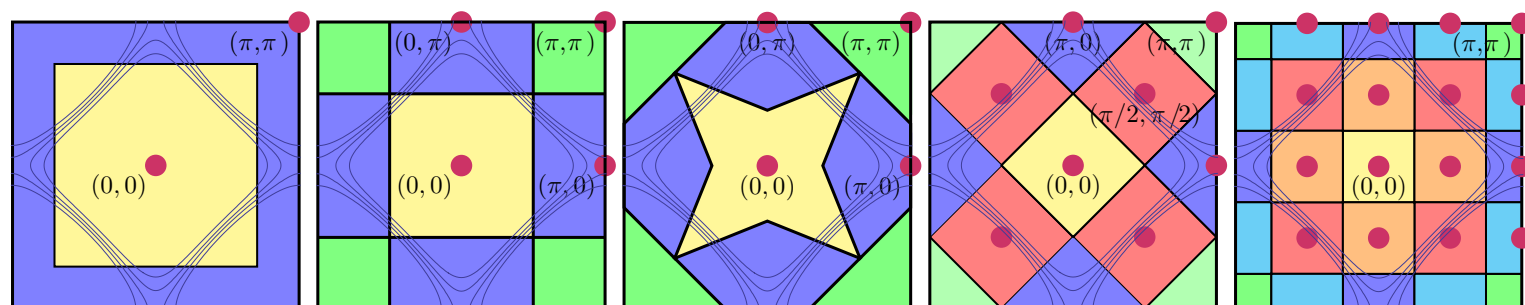
Typical 2d DCA clusters with 2, 4, 4, 8, and 16 sites

Cluster DMFT – Impurity Solvers

$$\Sigma(k,\omega) = \sum_n \Sigma_n(\omega)\phi_n(k) \approx \sum_n^{N_c} \Sigma_n(\omega)\phi_n(k)$$

Algorithm that produces $\Sigma_n(\omega)$: Mapping onto an impurity problem & self-consistent hybridization with a "bath".

$$H_{\mathrm{QI}} = H_{\mathrm{loc}} + H_{\mathrm{hyb}} + H_{\mathrm{bath}}$$

$$H_{\mathrm{loc}} = \sum_i \epsilon_i (n_{i\uparrow} + n_{i\downarrow}) + U n_{i\uparrow} n_{i\downarrow}$$

$$H_{\mathrm{bath}} = \sum_{k\alpha} \epsilon_{k\alpha} c^\dagger_{k\alpha} c_{k\alpha}$$

$$H_{\mathrm{hyb}} = \sum_{k\alpha b} V_k^{\alpha b} c^\dagger_{k\alpha} d_b + H.c.$$

Requirements for an 'impurity solver' algorithm:

• Solve large cluster impurity problems, at and away from half filling, for small and large interactions (density-density), at finite temperature.

• No further approximations (Δτ - errors, bath discretization, ...).

E. Gull, P. Werner, O. Parcollet, M. Troyer, EPL 82, 57003 (2008)

Cluster DMFT – Impurity Solvers

$$\Sigma(k,\omega) = \sum_n \Sigma_n(\omega)\phi_n(k) \approx \sum_n^{N_c} \Sigma_n(\omega)\phi_n(k)$$

Algorithm that produces $\Sigma_n(\omega)$: Mapping onto an impurity problem & self-consistent hybridization with a "bath".

$$H_{\text{QI}} = H_{\text{loc}} + H_{\text{hyb}} + H_{\text{bath}}$$

$$H_{\text{loc}} = \sum_i \epsilon_i(n_{i\uparrow} + n_{i\downarrow}) + U n_{i\uparrow} n_{i\downarrow}$$

$$H_{\text{bath}} = \sum_{k\alpha} \epsilon_{k\alpha} c_{k\alpha}^\dagger c_{k\alpha}$$

$$H_{\text{hyb}} = \sum_{k\alpha b} V_k^{\alpha b} c_{k\alpha}^\dagger d_b + H.c.$$

Only Candidates: Continuous-Time quantum Monte Carlo algorithms. We use: Continuous-Time Auxiliary Field (CT-AUX) algorithm.

E. Gull, P. Werner, O. Parcollet, M. Troyer, EPL 82, 57003 (2008)

Continuous-Time quantum Monte Carlo impurity solvers

Diagrammatic expansion of the partition function of an impurity model in the interaction or the hybridization, sampling of the resulting series stochastically up to infinite order.

A. N. Rubtsov, V. V. Savkin, A. I. Lichtenstein, Phys. Rev. B 72 035122 (2005)

$$H_{\mathrm{QI}} = H_a + H_b$$

$$Z = \mathrm{Tr}\, T_\tau e^{-\beta H_a} \exp\left[-\int_0^\beta d\tau H_b(\tau)\right] = \sum_k (-1)^k \int_0^\beta d\tau_1 \ldots \int_{\tau_{k-1}}^\beta d\tau_k \mathrm{Tr}\left[e^{-\beta H_a} H_b(\tau_k) H_b(\tau_{k-1}) \ldots H_b(\tau_1)\right]$$

Hybridization Expansion

$$H_a = H_{\mathrm{loc}};$$

$$H_b = H_{\mathrm{hyb}} + H_{\mathrm{bath}}$$

Exponential scaling in size of local Hilbert space

Continuous-Time Auxiliary Field

$$H_a = H_{\mathrm{bath}} + H_{\mathrm{hyb}} + H_{\mathrm{loc}}^0;$$

$$H_b = H_{\mathrm{loc}}^I$$

Efficiency dependent on type of interaction in H_{loc}^I

P. Werner, A. Comanac, L. de Medici, M. Troyer, and A. J. Millis, Phys. Rev. Lett. 97, 076405 (2006)

E. Gull, P. Werner, O. Parcollet, M. Troyer, EPL 82, 57003 (2008)

Continuous-Time Auxiliary Field impurity solver

Auxiliary field decoupling of interaction term s=±1

$$1 - \frac{\beta U}{K}\left(n_{i\uparrow}n_{i\downarrow} - \frac{n_{i\uparrow} + n_{i\downarrow}}{2}\right) = \frac{1}{2}\sum_{s=\pm 1}\exp\left(\gamma s(n_{i\uparrow} - n_{i\downarrow})\right),$$

$$\cosh(\gamma) = 1 + \frac{U\beta}{2K}.$$

s =

$$Z = \sum_{k=0}^{\infty}\sum_{s_1,\cdots s_k=\pm 1}\int_0^\beta d\tau_1 \cdots \int_{\tau_{k-1}}^\beta d\tau_k \left(\frac{K}{2\beta}\right)^k Z_k(\{s_k, \tau_k\}),$$ **Partition function expansion**

$$Z_k(\{s_i, \tau_i\}) \equiv \mathrm{Tr}\prod_{i=k}^1 \exp(-\Delta\tau_i H_0)\exp(s_i\gamma(n_\uparrow - n_\downarrow)).$$

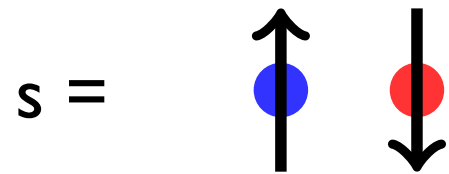**Compute trace of product of exponentials of one-body operators as determinant of matrix.**
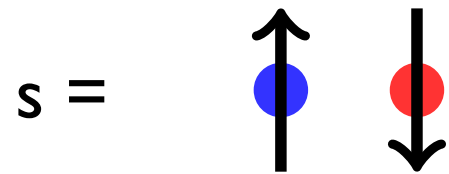
Stochastic sampling of diagrams of the partition function:

No truncation of expansion!

0 β

Continuous-Time Auxiliary Field impurity solver

Auxiliary field decoupling of interaction term s=±1

$$1 - \frac{\beta U}{K}\left(n_{i\uparrow}n_{i\downarrow} - \frac{n_{i\uparrow} + n_{i\downarrow}}{2}\right) = \frac{1}{2}\sum_{s=\pm 1}\exp\left(\gamma s(n_{i\uparrow} - n_{i\downarrow})\right),$$

$$\cosh(\gamma) = 1 + \frac{U\beta}{2K}.$$

s =

$$Z = \sum_{k=0}^{\infty}\sum_{s_1,\cdots s_k=\pm 1}\int_0^{\beta}d\tau_1\cdots\int_{\tau_{k-1}}^{\beta}d\tau_k\left(\frac{K}{2\beta}\right)^k Z_k(\{s_k,\tau_k\}),$$

Partition function expansion

$$Z_k(\{s_i,\tau_i\}) \equiv \mathrm{Tr}\prod_{i=k}^{1}\exp(-\Delta\tau_i H_0)\exp(s_i\gamma(n_\uparrow - n_\downarrow)).$$

Compute trace of product of exponentials of one-body operators as determinant of matrix.

Stochastic sampling of diagrams of the partition function:
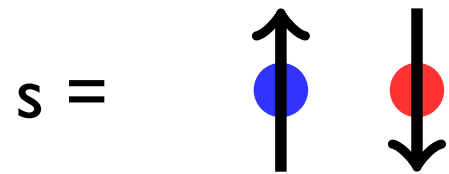
No truncation of expansion!

0   τ_1 β

Continuous-Time Auxiliary Field impurity solver

Auxiliary field decoupling of interaction term s=±1

$$1 - \frac{\beta U}{K}\left(n_{i\uparrow}n_{i\downarrow} - \frac{n_{i\uparrow} + n_{i\downarrow}}{2}\right) = \frac{1}{2}\sum_{s=\pm 1}\exp\left(\gamma s(n_{i\uparrow} - n_{i\downarrow})\right),$$

$$\cosh(\gamma) = 1 + \frac{U\beta}{2K}.$$

s =

$$Z = \sum_{k=0}^{\infty}\sum_{s_1,\cdots s_k = \pm 1}\int_0^\beta d\tau_1 \cdots \int_{\tau_{k-1}}^\beta d\tau_k \left(\frac{K}{2\beta}\right)^k Z_k(\{s_k, \tau_k\}),$$
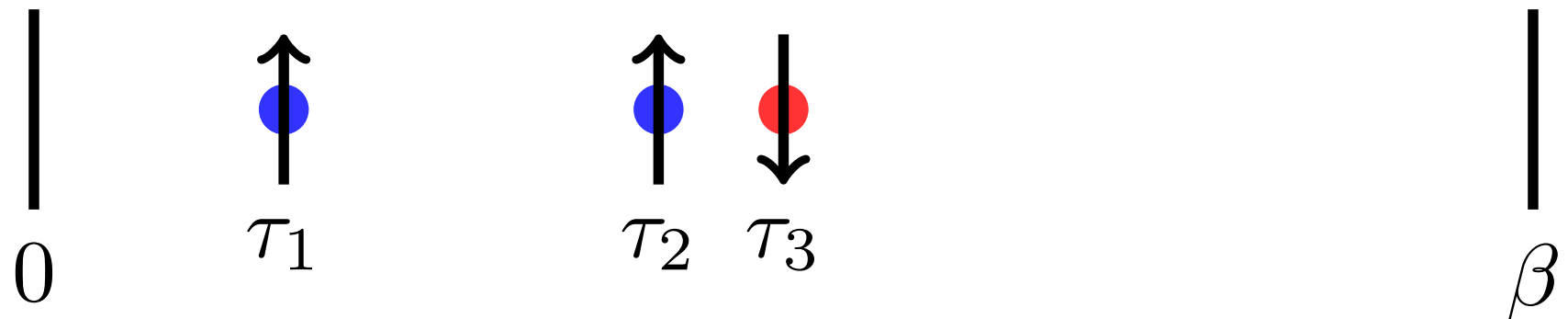
Partition function expansion

$$Z_k(\{s_i, \tau_i\}) \equiv \mathrm{Tr}\prod_{i=k}^{1}\exp(-\Delta\tau_i H_0)\exp(s_i\gamma(n_\uparrow - n_\downarrow)).$$

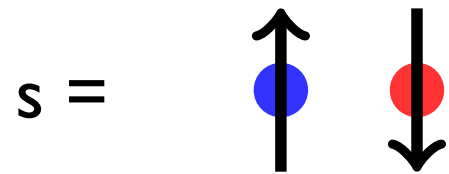**Compute trace of product of exponentials of one-body operators as determinant of matrix.**

Stochastic sampling of diagrams of the partition function:

No truncation of expansion!

0 τ_1 τ_2 β

Continuous-Time Auxiliary Field impurity solver

Auxiliary field decoupling of interaction term s=±1

$$1 - \frac{\beta U}{K}\left(n_{i\uparrow}n_{i\downarrow} - \frac{n_{i\uparrow} + n_{i\downarrow}}{2}\right) = \frac{1}{2}\sum_{s=\pm 1}\exp\left(\gamma s(n_{i\uparrow} - n_{i\downarrow})\right),$$

$$\cosh(\gamma) = 1 + \frac{U\beta}{2K}.$$

s =

$$Z = \sum_{k=0}^{\infty}\sum_{s_1,\cdots s_k=\pm 1}\int_0^{\beta}d\tau_1\cdots\int_{\tau_{k-1}}^{\beta}d\tau_k\left(\frac{K}{2\beta}\right)^k Z_k(\{s_k,\tau_k\}),$$

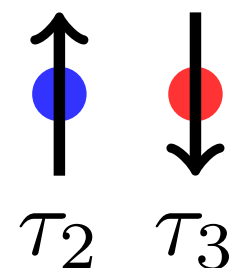**Partition function expansion**

$$Z_k(\{s_i,\tau_i\}) \equiv \mathrm{Tr}\prod_{i=k}^{1}\exp(-\Delta\tau_i H_0)\exp(s_i\gamma(n_\uparrow - n_\downarrow)).$$

Compute trace of product of exponentials of one-body operators as determinant of matrix.

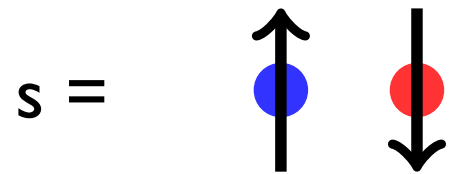**Stochastic sampling of diagrams of the partition function:**

No truncation of expansion!

0 τ_1 τ_2 τ_3 β

Continuous-Time Auxiliary Field impurity solver

Auxiliary field decoupling of interaction term s=±1

$$1 - \frac{\beta U}{K}\left(n_{i\uparrow}n_{i\downarrow} - \frac{n_{i\uparrow}+n_{i\downarrow}}{2}\right) = \frac{1}{2}\sum_{s=\pm 1}\exp\left(\gamma s(n_{i\uparrow}-n_{i\downarrow})\right),$$

$$\cosh(\gamma) = 1 + \frac{U\beta}{2K}.$$

s =

$$Z = \sum_{k=0}^{\infty}\sum_{s_1,\cdots s_k=\pm 1}\int_0^{\beta}d\tau_1\cdots\int_{\tau_{k-1}}^{\beta}d\tau_k\left(\frac{K}{2\beta}\right)^k Z_k(\{s_k,\tau_k\}),$$ **Partition function expansion**
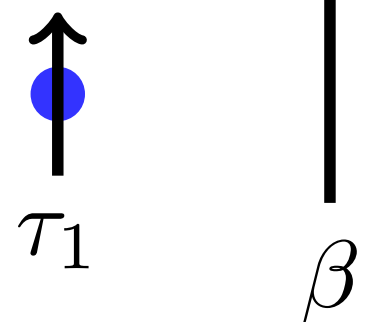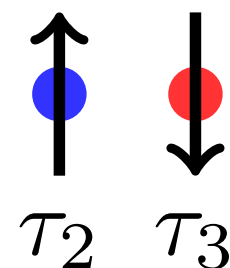
$$Z_k(\{s_i,\tau_i\}) \equiv \mathrm{Tr}\prod_{i=k}^{1}\exp(-\Delta\tau_i H_0)\exp(s_i\gamma(n_\uparrow - n_\downarrow)).$$

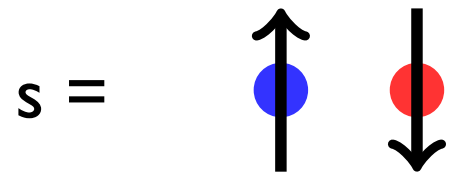**Compute trace of product of exponentials of one-body operators as determinant of matrix.**

Stochastic sampling of diagrams of the partition function:

No truncation of expansion!

0 τ_2 τ_3 β

Continuous-Time Auxiliary Field impurity solver

Auxiliary field decoupling of interaction term s=±1

$$1 - \frac{\beta U}{K}\left(n_{i\uparrow}n_{i\downarrow} - \frac{n_{i\uparrow} + n_{i\downarrow}}{2}\right) = \frac{1}{2}\sum_{s=\pm 1}\exp\left(\gamma s(n_{i\uparrow} - n_{i\downarrow})\right),$$

$$\cosh(\gamma) = 1 + \frac{U\beta}{2K}.$$

s =

$$Z = \sum_{k=0}^{\infty}\sum_{s_1,\cdots s_k=\pm 1}\int_0^{\beta}d\tau_1\cdots\int_{\tau_{k-1}}^{\beta}d\tau_k\left(\frac{K}{2\beta}\right)^k Z_k(\{s_k,\tau_k\}),$$

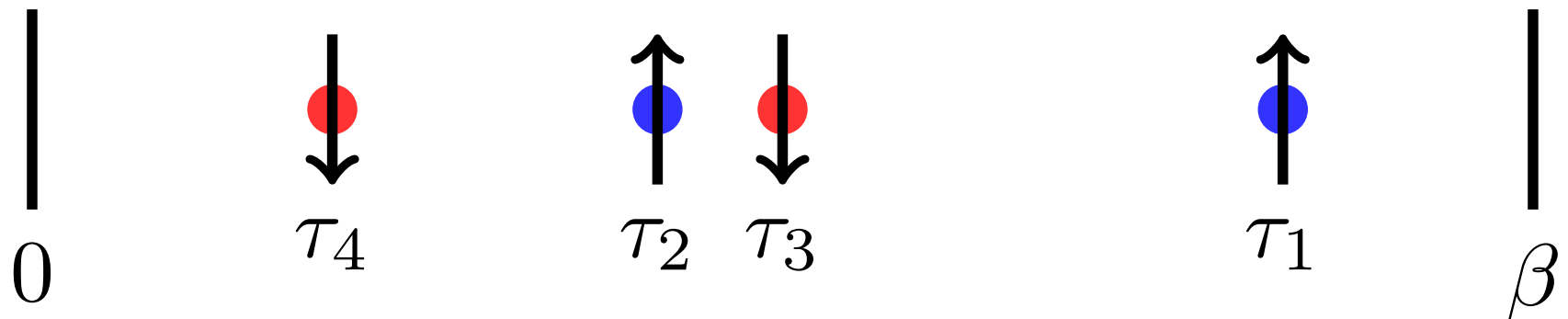**Partition function expansion**

$$Z_k(\{s_i,\tau_i\}) \equiv \mathrm{Tr}\prod_{i=k}^{1}\exp(-\Delta\tau_i H_0)\exp(s_i\gamma(n_\uparrow - n_\downarrow)).$$

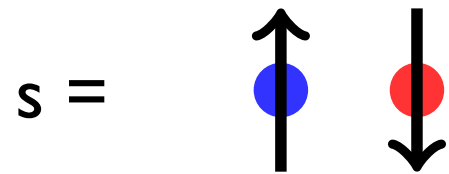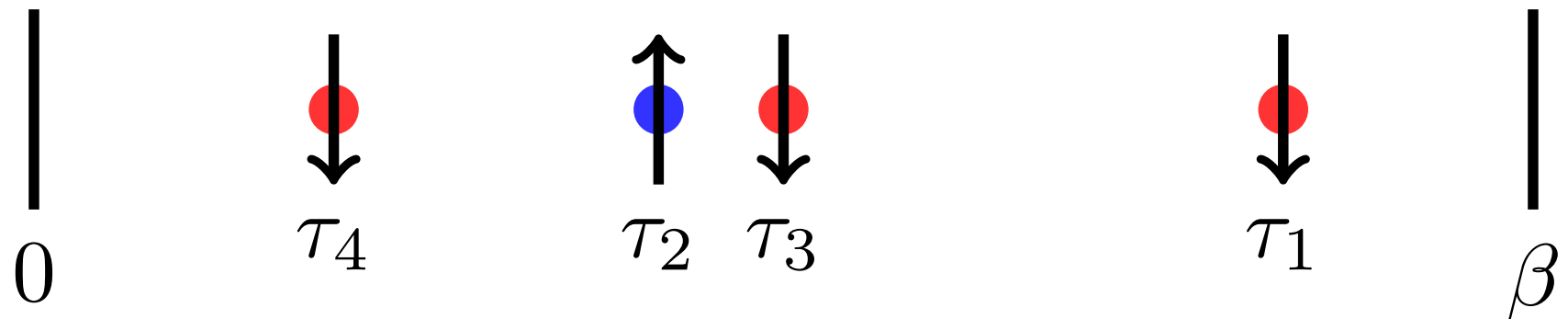**Compute trace of product of exponentials of one-body operators as determinant of matrix.**

Stochastic sampling of diagrams of the partition function:

No truncation of expansion!

0 τ_2 τ_3 τ_1 β

Continuous-Time Auxiliary Field impurity solver

Auxiliary field decoupling of interaction term s=±1

$$1 - \frac{\beta U}{K}\left(n_{i\uparrow}n_{i\downarrow} - \frac{n_{i\uparrow}+n_{i\downarrow}}{2}\right) = \frac{1}{2}\sum_{s=\pm1}\exp\left(\gamma s(n_{i\uparrow}-n_{i\downarrow})\right),$$

$$\cosh(\gamma) = 1 + \frac{U\beta}{2K}.$$

s =

$$Z = \sum_{k=0}^{\infty}\sum_{s_1,\cdots s_k=\pm1}\int_0^\beta d\tau_1\cdots\int_{\tau_{k-1}}^\beta d\tau_k\left(\frac{K}{2\beta}\right)^k Z_k(\{s_k,\tau_k\}),$$

Partition function expansion

$$Z_k(\{s_i,\tau_i\}) \equiv \mathrm{Tr}\prod_{i=k}^1\exp(-\Delta\tau_i H_0)\exp(s_i\gamma(n_\uparrow-n_\downarrow)).$$

Compute trace of product of exponentials of one-body operators as determinant of matrix.

Stochastic sampling of diagrams of the partition function:

No truncation of expansion!

0 τ_4 τ_2 τ_3 τ_1 β

Continuous-Time Auxiliary Field impurity solver

Auxiliary field decoupling of interaction term s=±1

$$1 - \frac{\beta U}{K}\left(n_{i\uparrow}n_{i\downarrow} - \frac{n_{i\uparrow}+n_{i\downarrow}}{2}\right) = \frac{1}{2}\sum_{s=\pm 1}\exp\left(\gamma s(n_{i\uparrow}-n_{i\downarrow})\right),$$

$$\cosh(\gamma) = 1 + \frac{U\beta}{2K}.$$

s =

$$Z = \sum_{k=0}^{\infty}\sum_{s_1,\cdots s_k=\pm 1}\int_0^\beta d\tau_1 \cdots \int_{\tau_{k-1}}^\beta d\tau_k \left(\frac{K}{2\beta}\right)^k Z_k(\{s_k,\tau_k\}),$$

Partition function expansion

$$Z_k(\{s_i,\tau_i\}) \equiv \mathrm{Tr}\prod_{i=k}^{1}\exp(-\Delta\tau_i H_0)\exp(s_i\gamma(n_\uparrow - n_\downarrow)).$$

Compute trace of product of exponentials of one-body operators as determinant of matrix.

Stochastic sampling of diagrams of the partition function:

No truncation of expansion!

0 τ_4 τ_2 τ_3 τ_1 β

Sub-Matrix updates

Standard updates in auxiliary field impurity solvers: rank one operations (ger), $O(N^2)$ operations for $O(N^2)$ data: dominated by data access.

$$N'_{ij} \leftarrow N_{ij} + (G_{ip} - \delta_{ip})\lambda_p \times [\, N_{pj} \,]$$

Sub-Matrix updates: based on matrix (gemm) operations: $O(N^3)$ operations on $O(N^2)$ data: runs at speed of (fast) CPU/Cache.

$$N_{ij}^{q+1} \leftarrow D_i^{-1}(N_{ij}^q - G_{ip_k}^q \times [\Gamma_{p_k p_l}^{-1}] \times [\, N_{p_l j} \,])$$
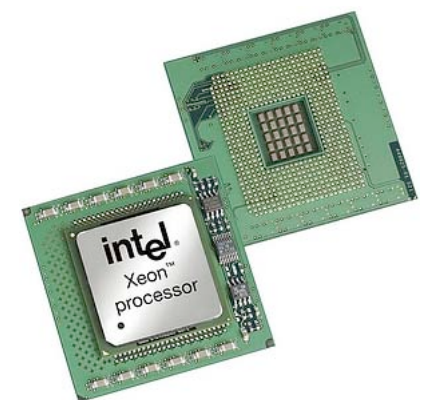
Linear algebra reformulated, overhead grows with size of Γ but operations 10x faster

Technical Challenges

Scaling: determines how large clusters are accessible; whether the infinite cluster size extrapolation is possible in practice.

Weak Scaling

Scaling as a function of **problem size** (cluster size, interaction strength, inverse temperature).
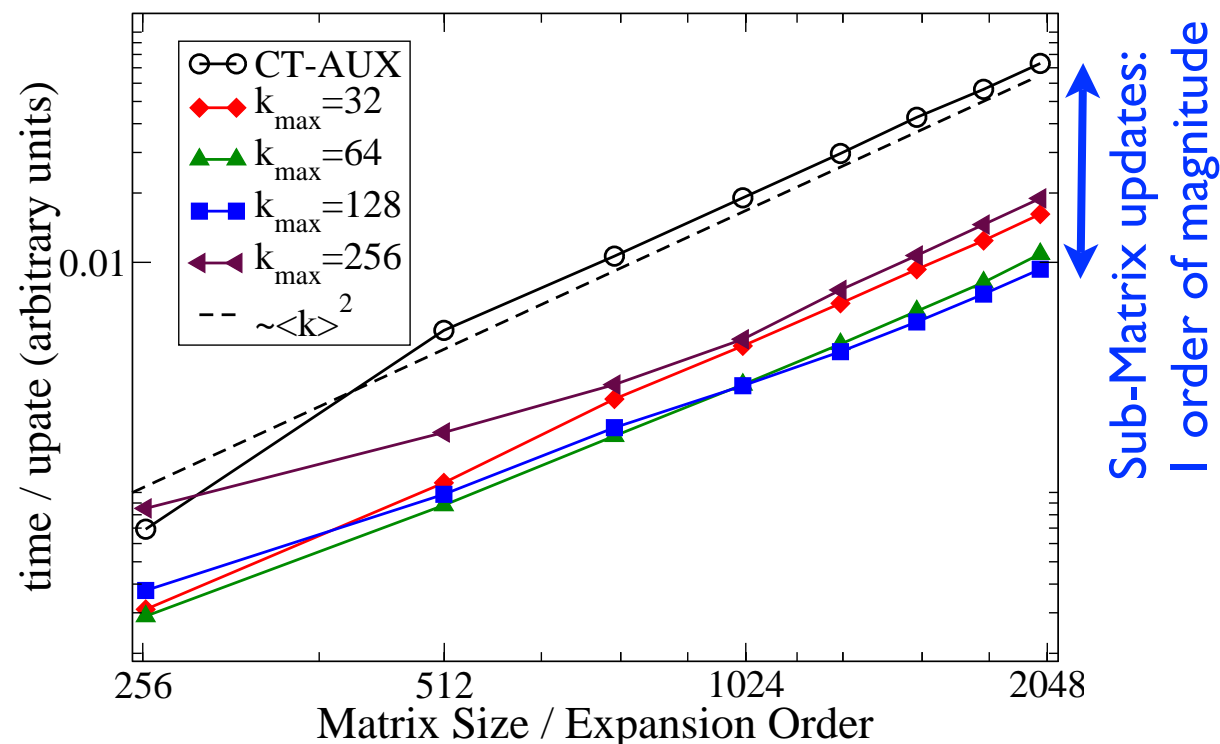
Strong scaling

Scaling as a function of **resources**: Time to solution for a typical problem (16 site cluster, U/t = 8, beta t=10 and 20)
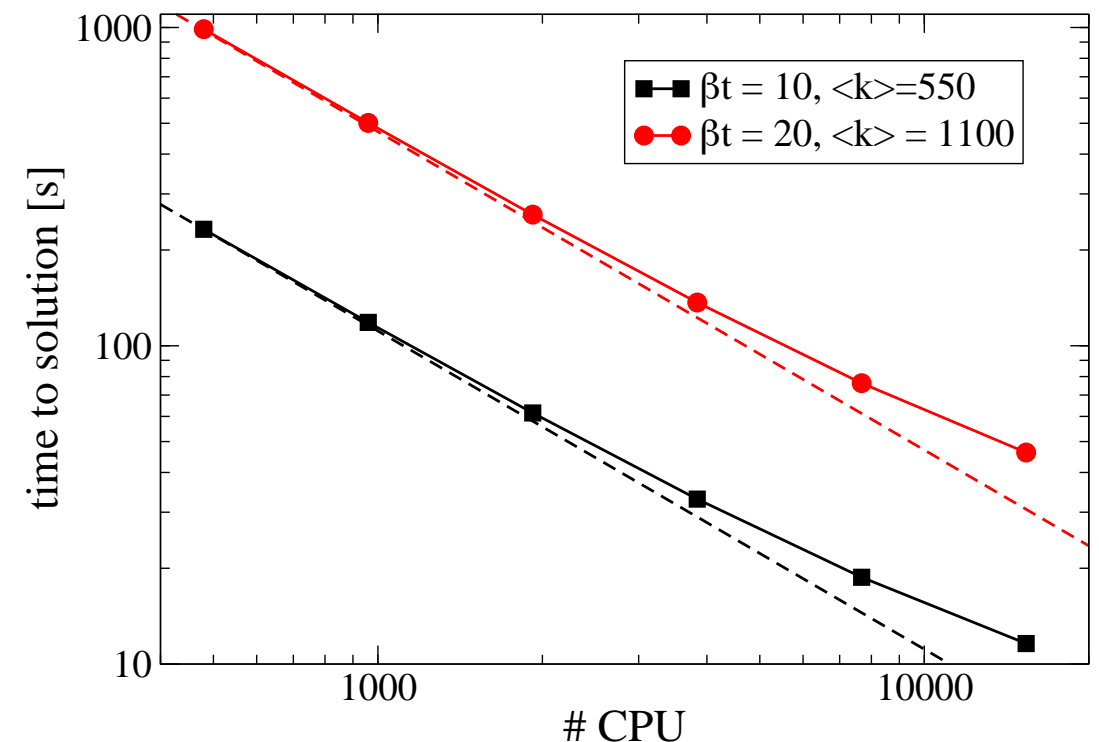
All results from now on: Obtained with ≤128 CPUs, ≤2h per iteration.

Extrapolation procedure

Solve quantum impurity model self-consistently for a range of cluster sizes:

18   36   48   56   64   84   100
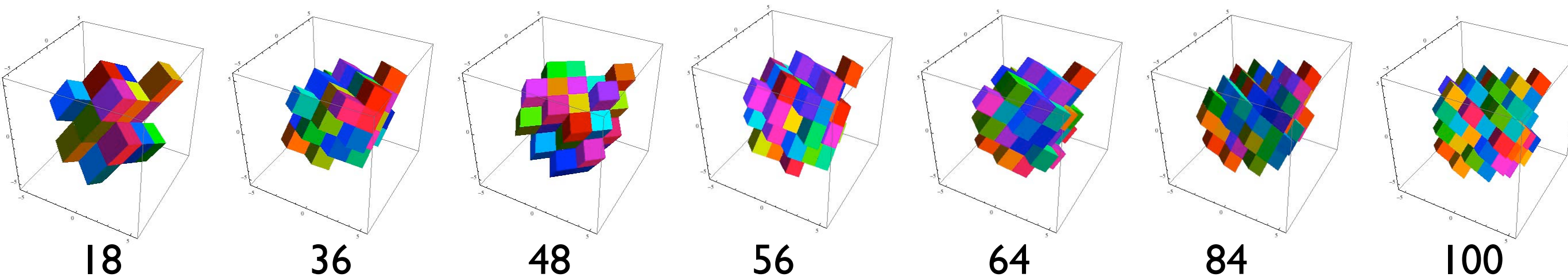
Compute thermodynamics: energy, density, entropy, free energy, double occupancy, spin correlation functions, …: Results and error estimates for a finite size system.

Extrapolate observable estimate to the infinite system size limit using known finite size scaling:

Results for finite clusters without extrapolations are not accurate!
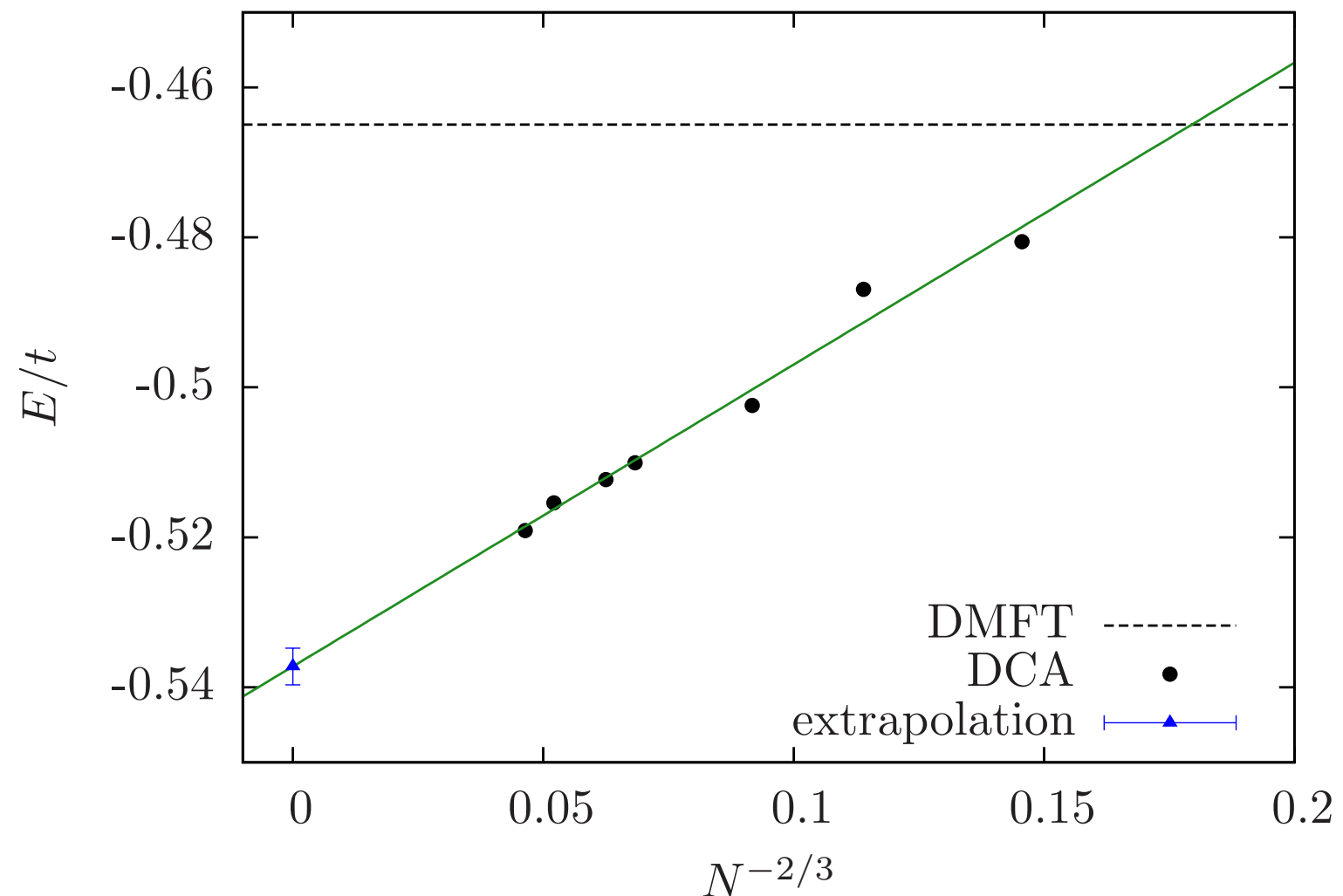
Cluster DMFT vs Lattice Methods

What is gained by embedding the cluster into a self-consistent bath (vs lattice)?

- Convergence in DCA seems to be faster: series 64-84-100 sites comparable to $6^3, 8^3, 10^3$ sites in lattice simulation.

- Sign problem is better:

Sign problem away from 1/2 filling (U=8, 64-site cluster at filling 0.2)

DCA ●
free cluster ▼
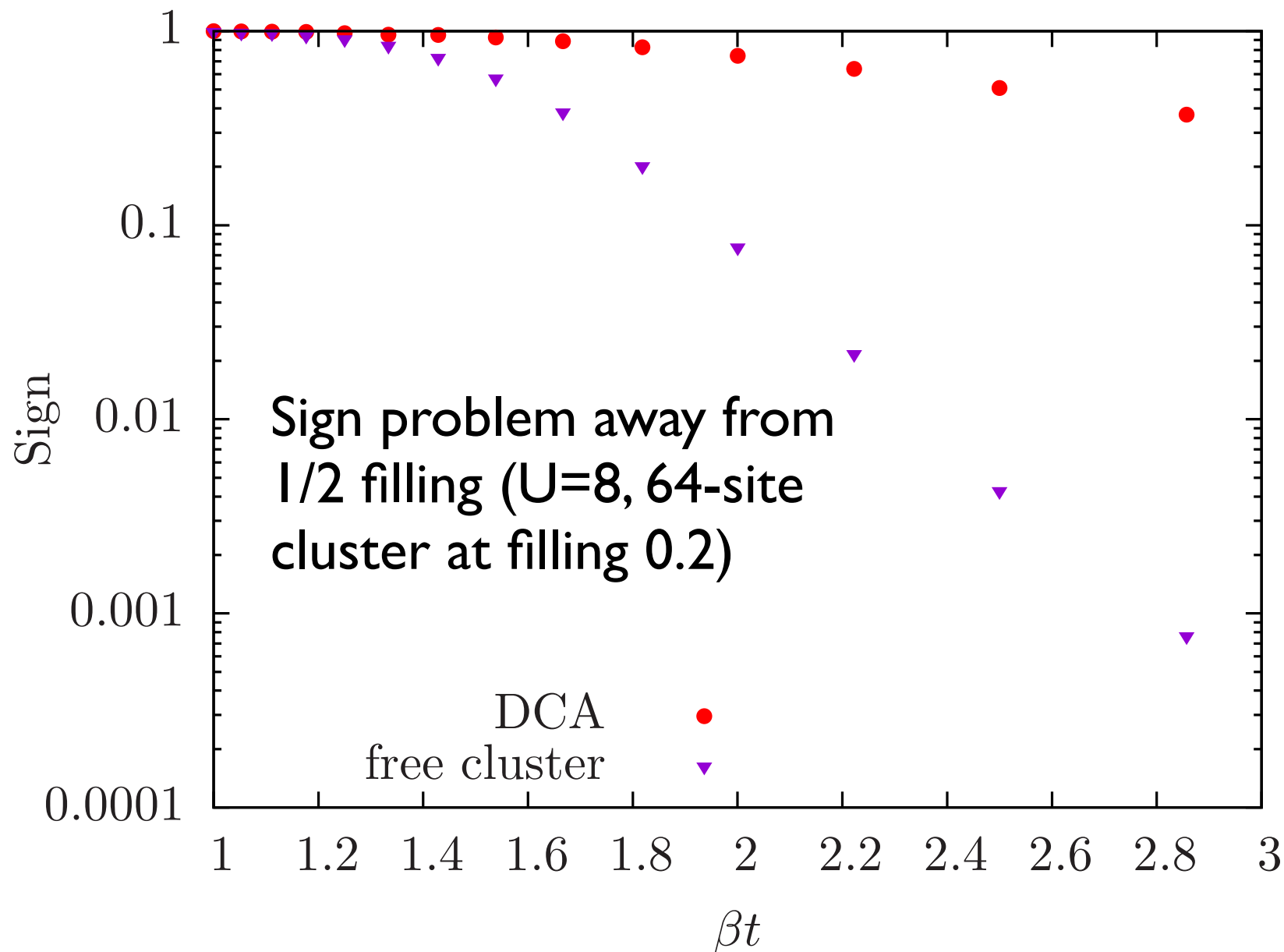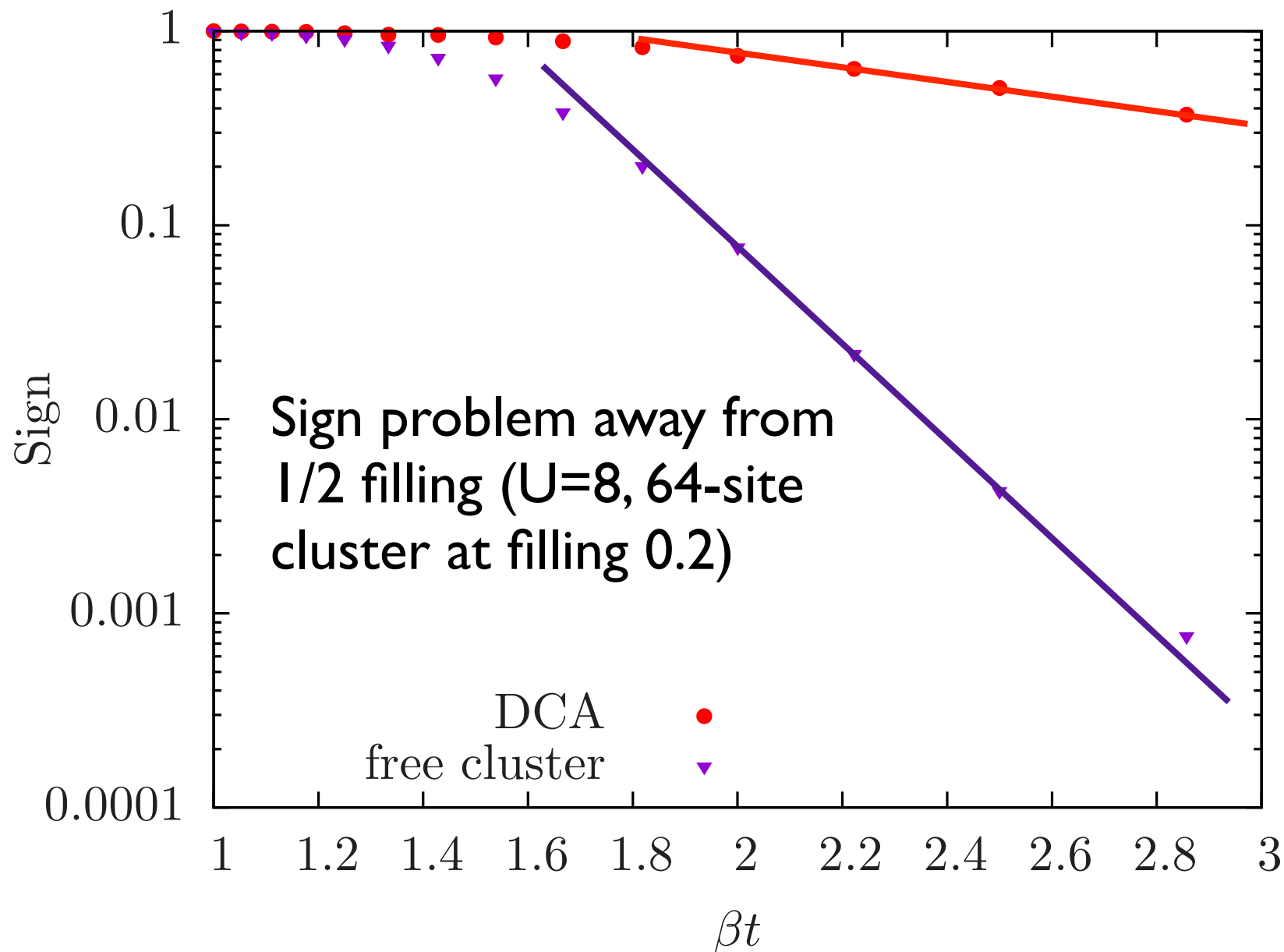
Slope of drop of sign for cluster calculation is different from lattice calculation

First self-consistency iteration (starting from free solution): lattice problem with periodic boundary conditions. Sign problem for lattice problem : the same in BSS / CT-AUX

DCA Results: The 3D Hubbard Model

P. R. C. Kent, M. Jarrell, T. A. Maier, and Th. Pruschke, Phys. Rev. B 72, 060411(R) (2005)
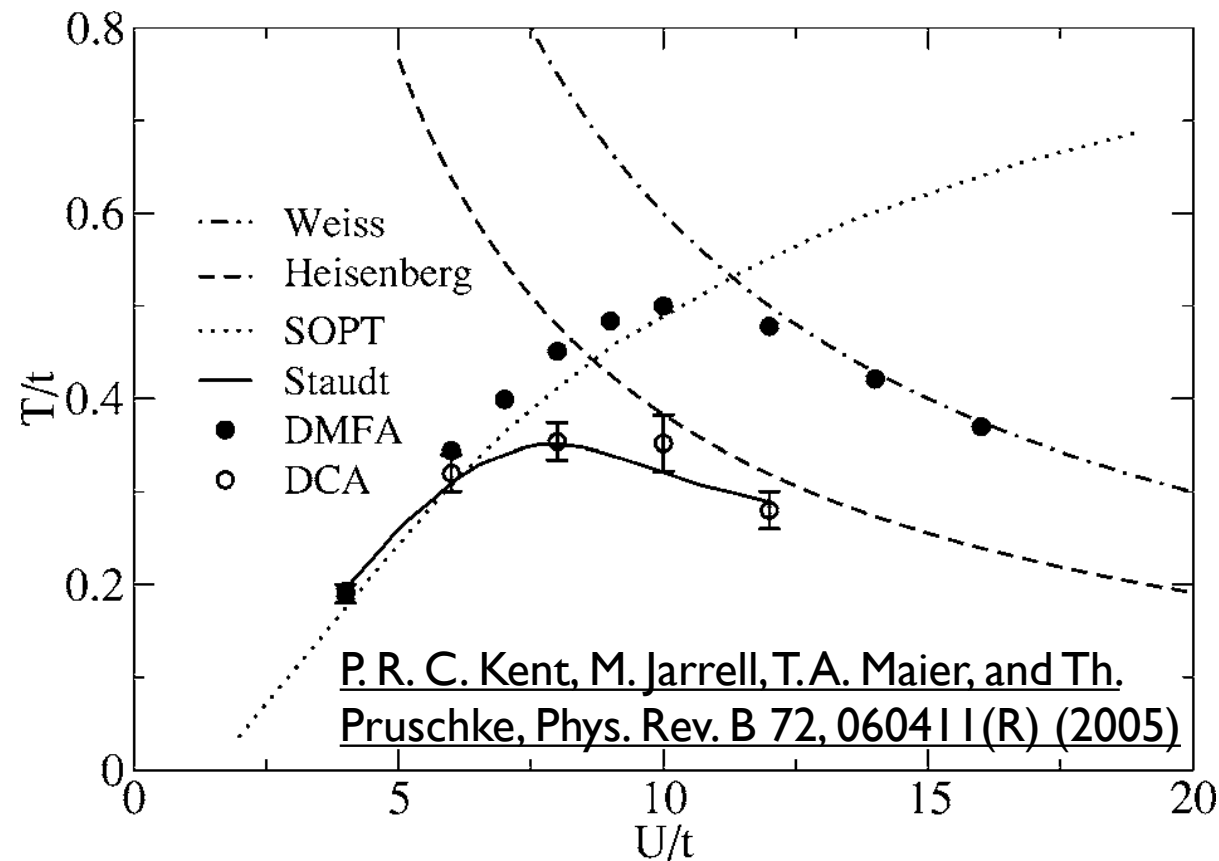
At half filling: Antiferromagnetic state below T_N. Single site DMFT transition temperature too high.

Anything below (or very near) T_N not considered in this study!

Away from half filling: ?

In 2d: isotropic Fermi Liquid regime in two dimensions for small fillings (n ~ 0.7). Cluster corrections important for larger fillings

Cluster sign problem far away from half filling is much worse than close to half filling!

2d results: momentum independent behavior for low filling.
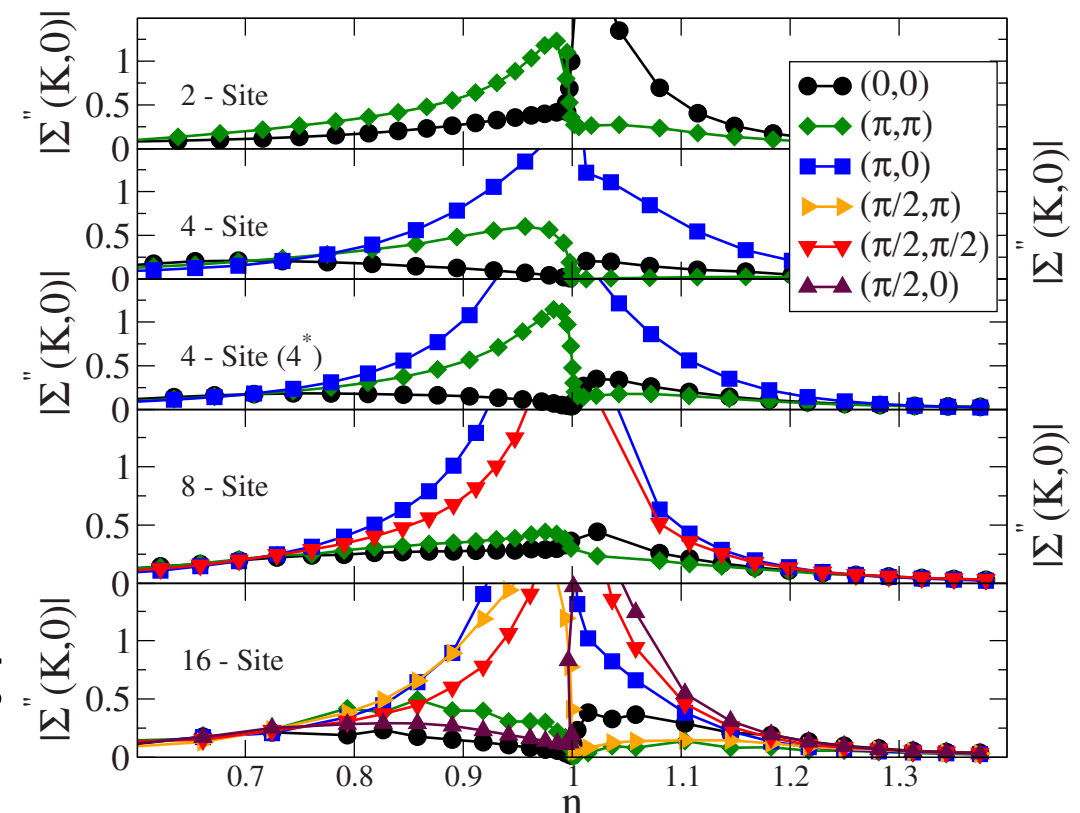
DCA Results: The 3D Hubbard Model

Comparison HTSE / DCA?
(6th, 8th, 10th order)

HTSE order by order convergence: at U=8 correct down to T ~ 1.6t (at half filling). Worse away from half filling.

Agreement of 10th order HTSE with DCA down to T~1.4t.

See also: in depth analysis of HTSE & DMFT by L. De Leo, J.S. Bernier, C. Kollath, A. Georges, V. W. Scarola, arXiv: 1009.2761
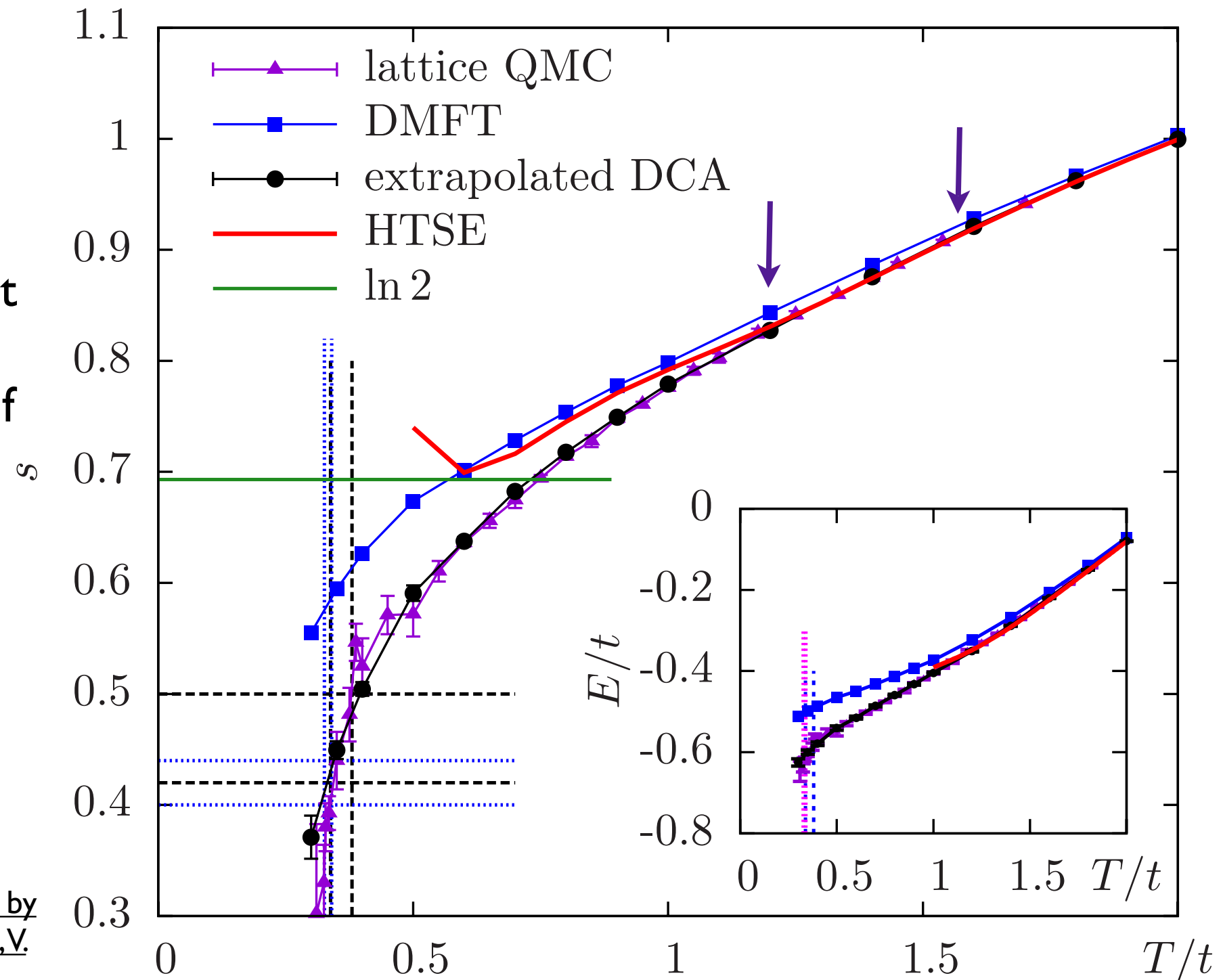
DCA Results: The 3D Hubbard Model

How well does single site DMFT work?
(Single Site, PM self consistency)

First deviations at half filling are visible
at T ~ 1.6t [AFM T_N at ~0.5t]
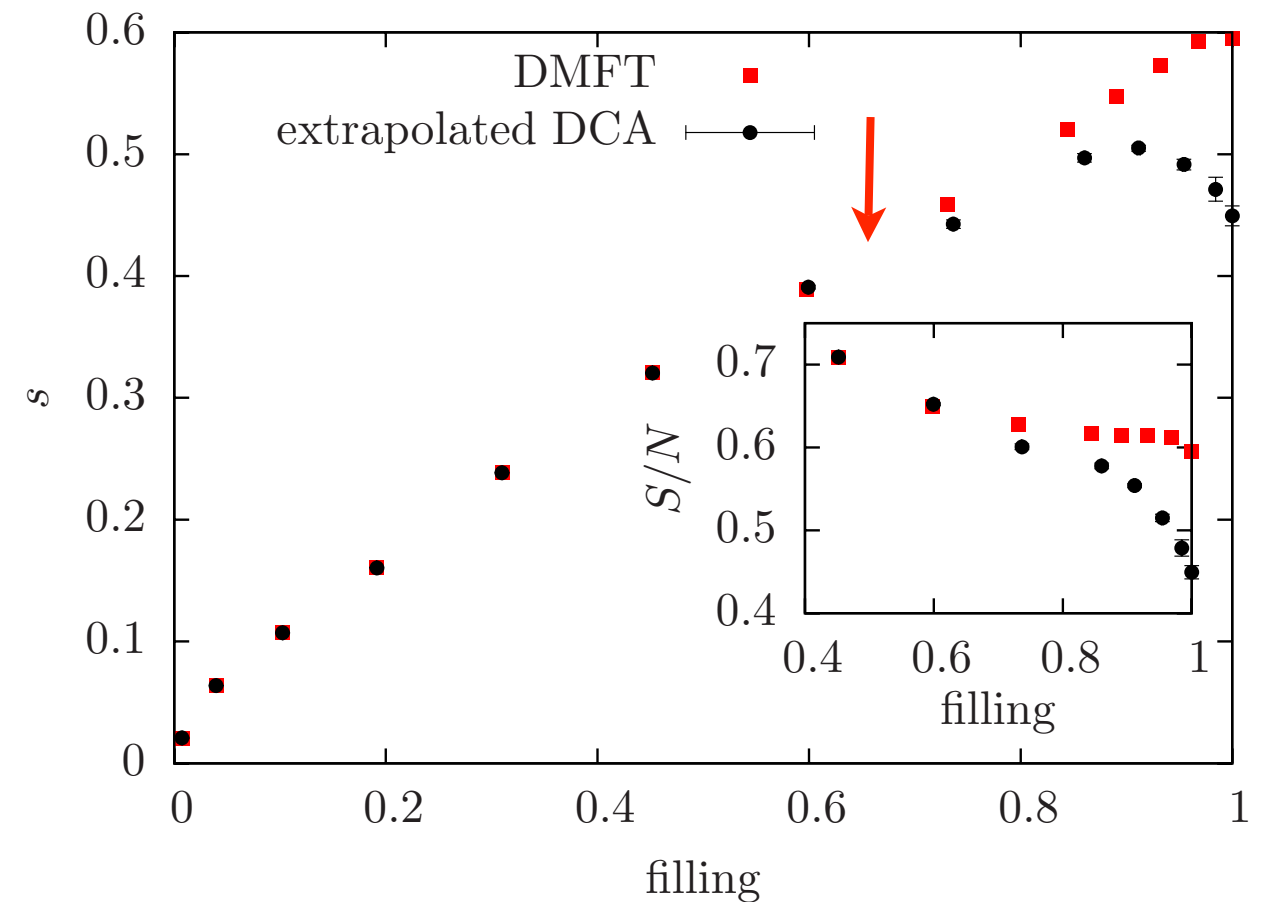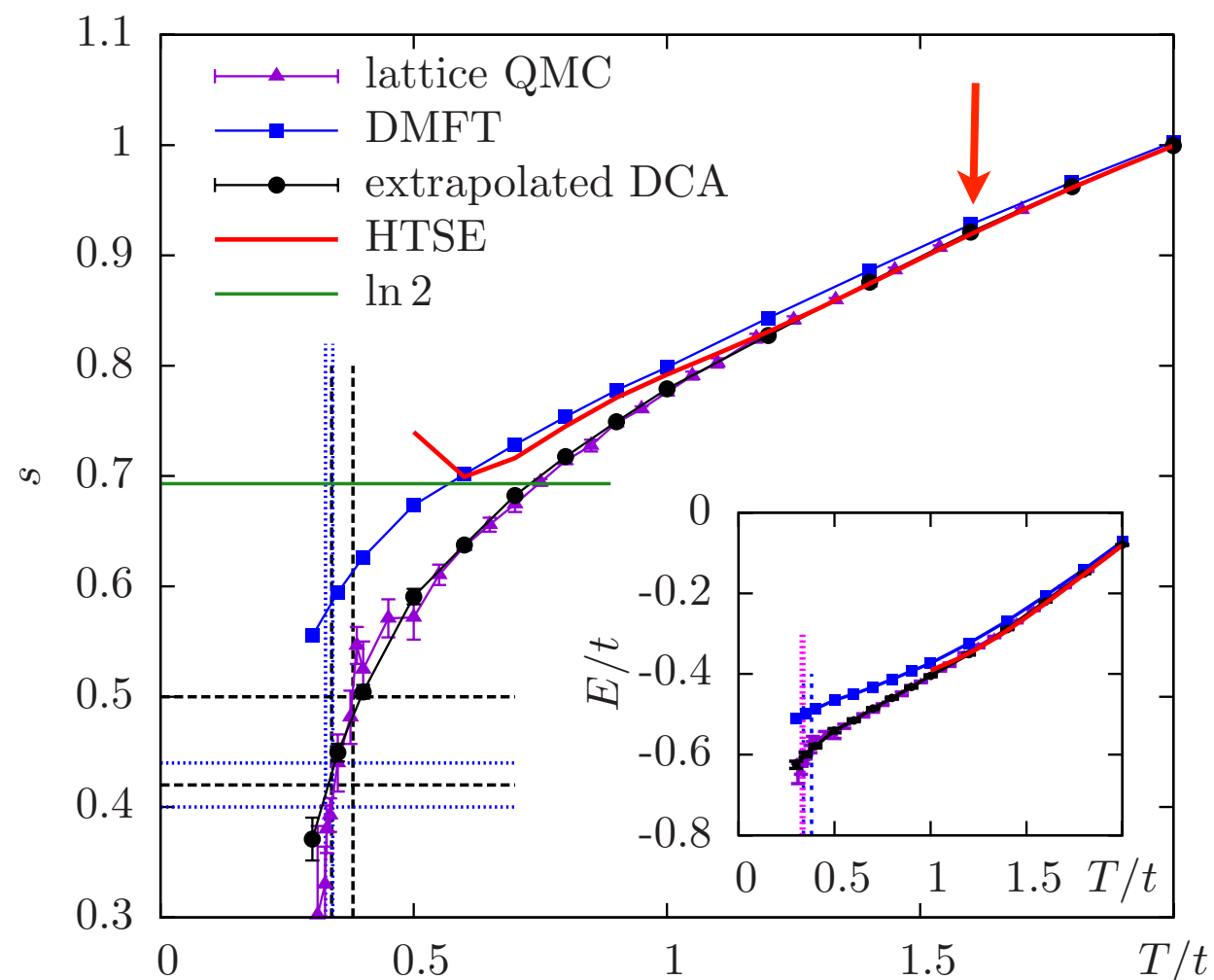
Away from half filling, for n ≤ 0.7: same behavior as in 2D; DMFT is exact, no momentum dependence of the self energy:

$$\Sigma(k,\omega) = \sum_n \Sigma_n(\omega)\phi_n(k) = \Sigma_{\mathrm{DMFT}}(\omega)$$

n < 0.7

DCA Results: The 3D Hubbard Model

Everywhere else: Non-local (momentum dependent) physics beyond DMFT is important.
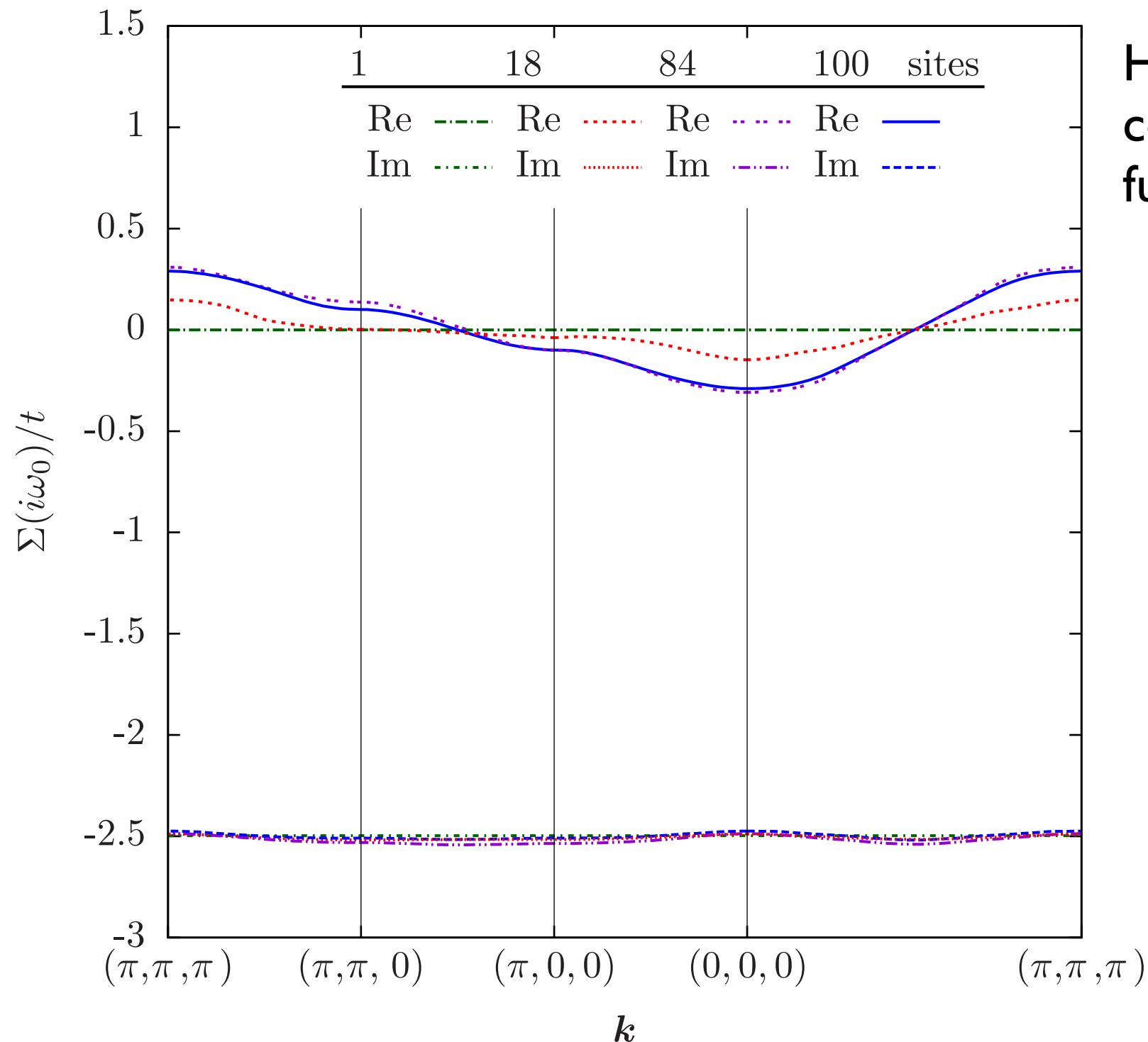
High temperature $T/t = 1$: Exact convergence of the self energy as a function of cluster size.

DCA Results: The 3D Hubbard Model

Everywhere else: Non-local (momentum dependent) physics beyond DMFT is important.
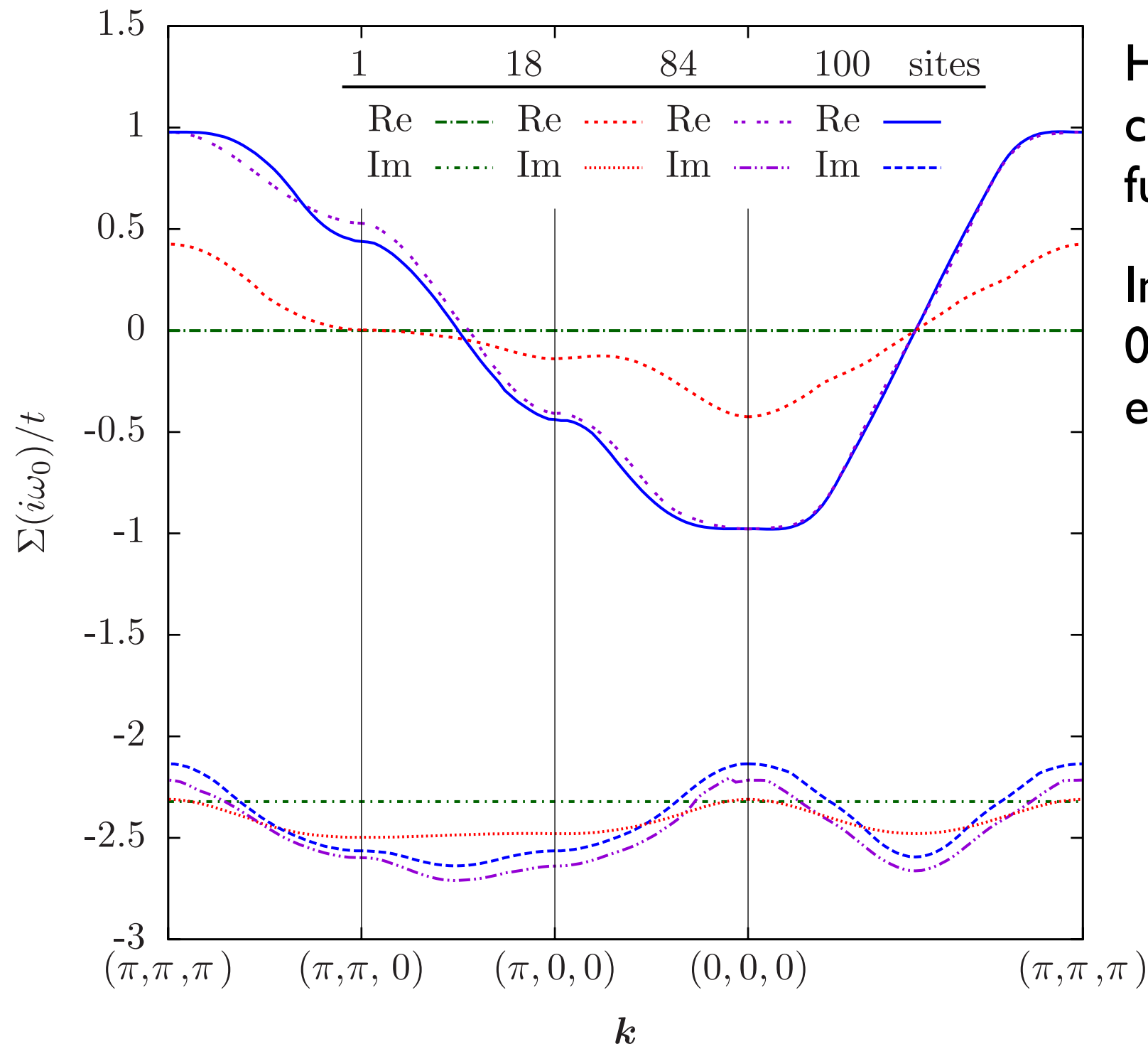
High temperature T/t = 1: Exact convergence of the self energy as a function of cluster size.

Intermediate temperature T/t = 0.5: Convergence visible, extrapolation needed.

DCA Results: The 3D Hubbard Model

Everywhere else: Non-local (momentum dependent) physics beyond DMFT is important.
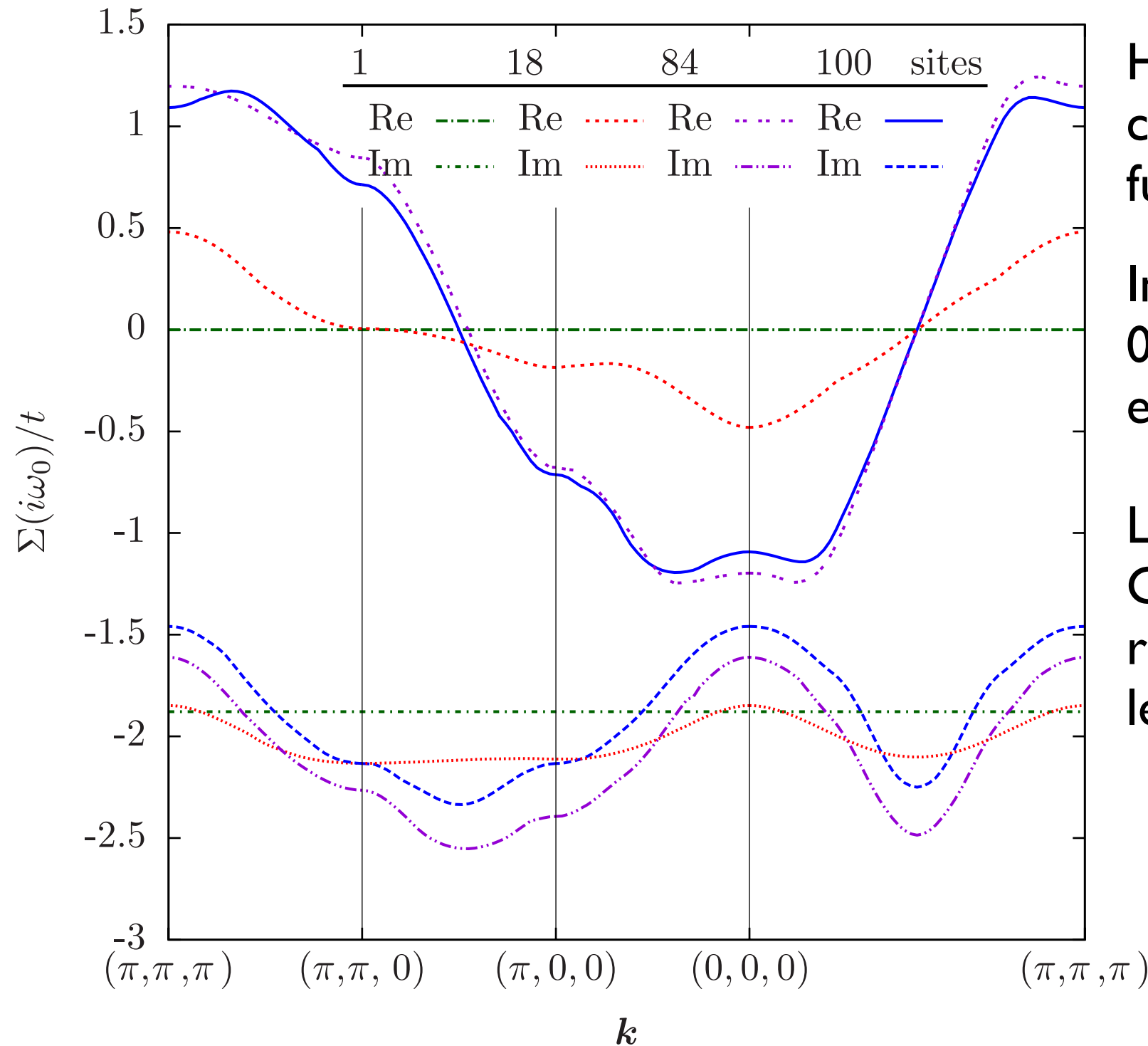
High temperature T/t = 1: Exact convergence of the self energy as a function of cluster size.

Intermediate temperature T/t = 0.5: Convergence visible, extrapolation needed.

Low temperature T/t = 0.35: Convergence not obvious, critical regime with diverging correlation length not well captured.

DCA Results: The 3D Hubbard Model

Everywhere else: Non-local (momentum dependent) physics beyond DMFT is important.
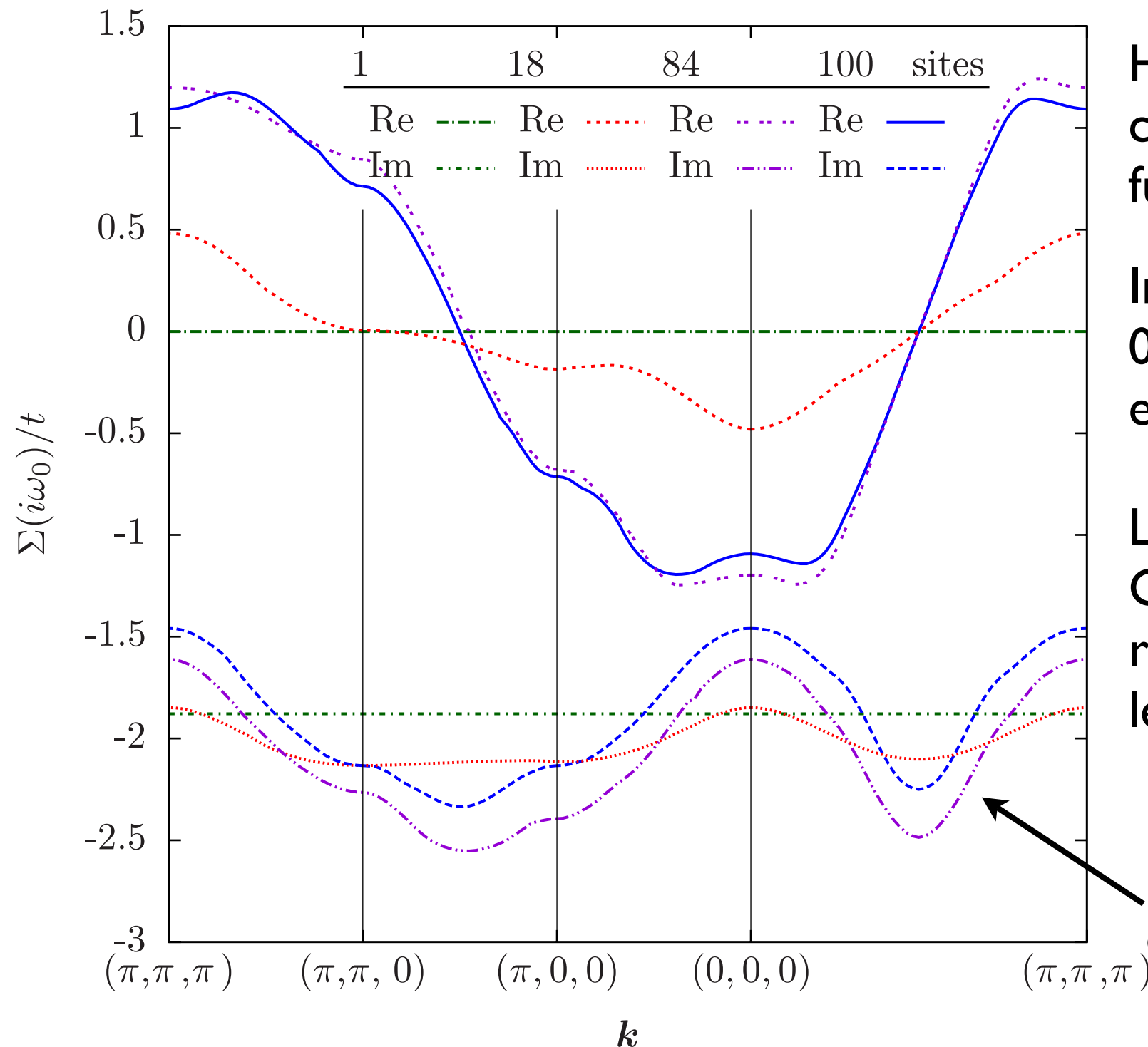
High temperature T/t = 1: Exact convergence of the self energy as a function of cluster size.

Intermediate temperature T/t = 0.5: Convergence visible, extrapolation needed.

Low temperature T/t = 0.35: Convergence not obvious, critical regime with diverging correlation length not well captured.

Non-trivial momentum dependence!

DCA Results: The 3D Hubbard Model

Failure (?) of the method for larger interactions / lower temperatures

Monte Carlo errors much smaller than symbol size!!
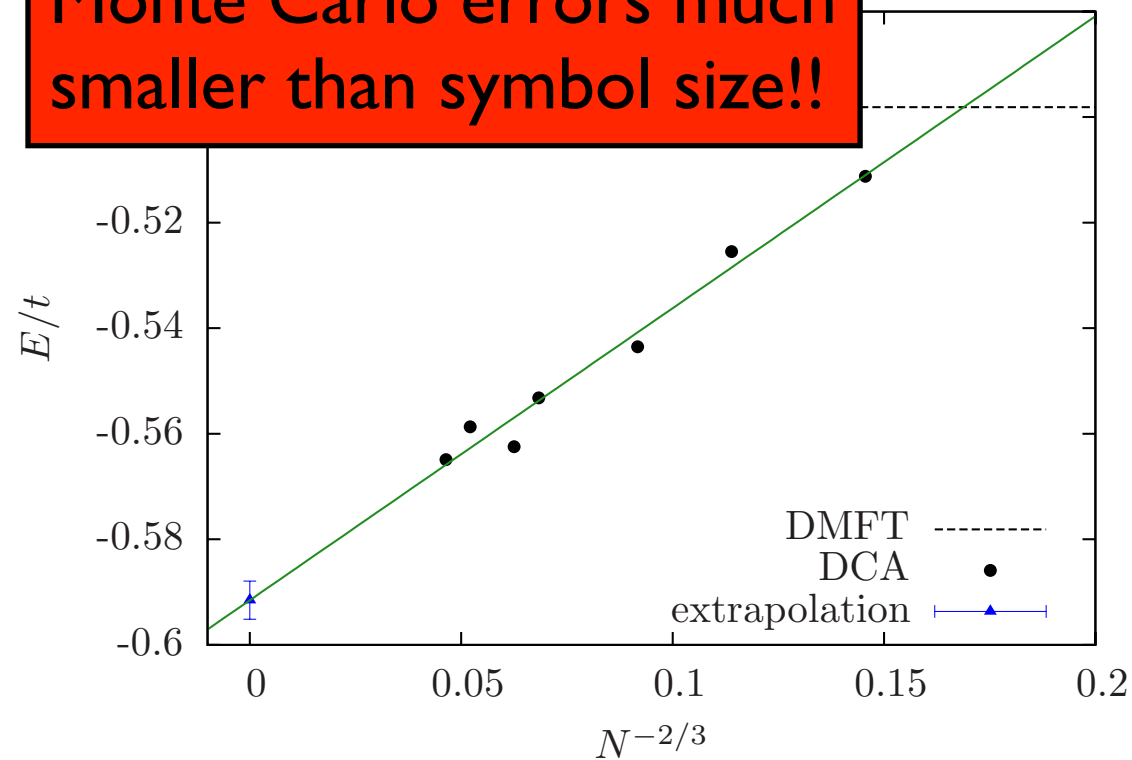
Finite size extrapolation of the energies still ~ OK
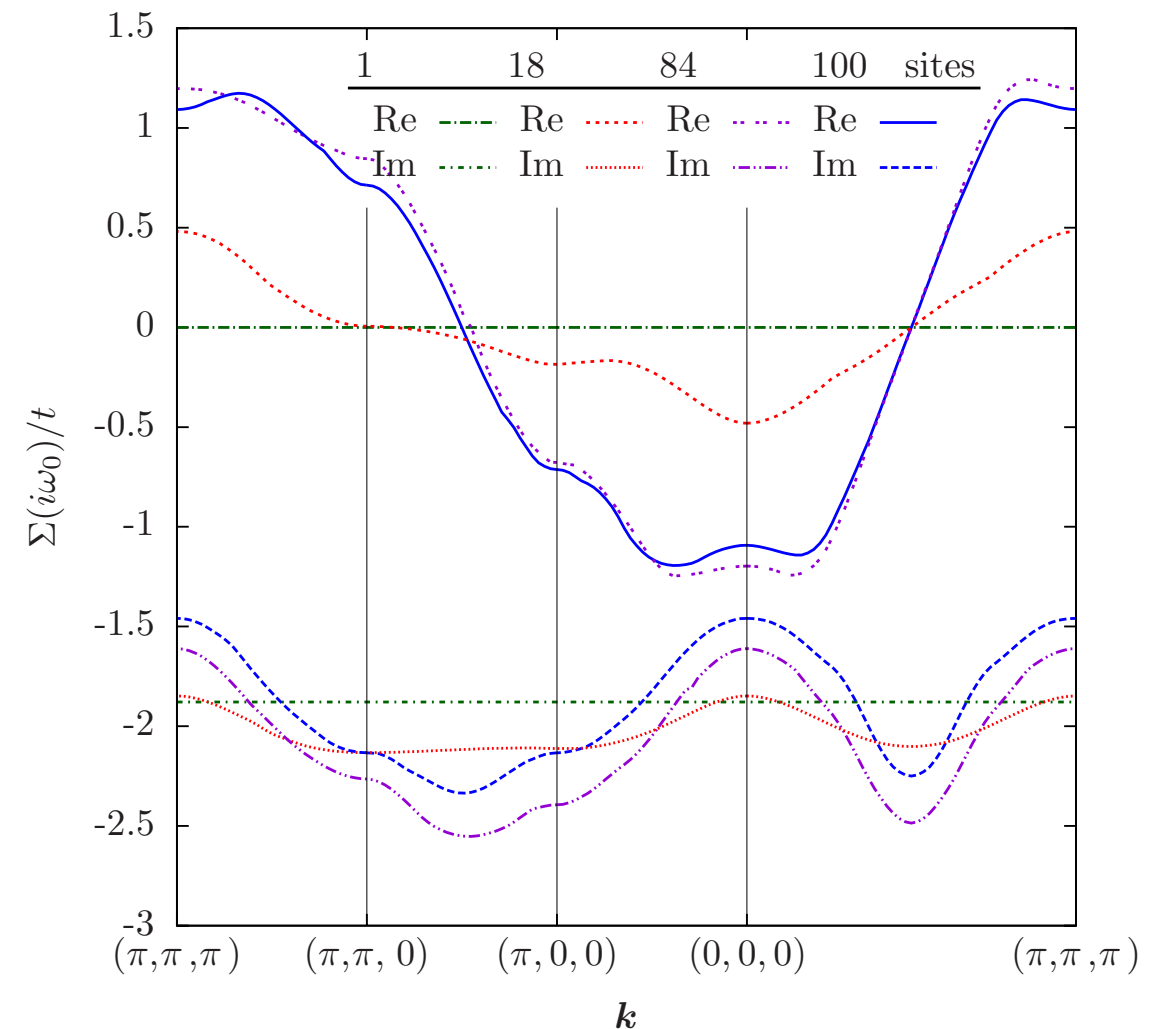
Extrapolation of the self energy not ok, would need even larger clusters (or a *next generation method?*)

DCA Results: The 3D Hubbard Model

Double occupancies / deviation from DMFT
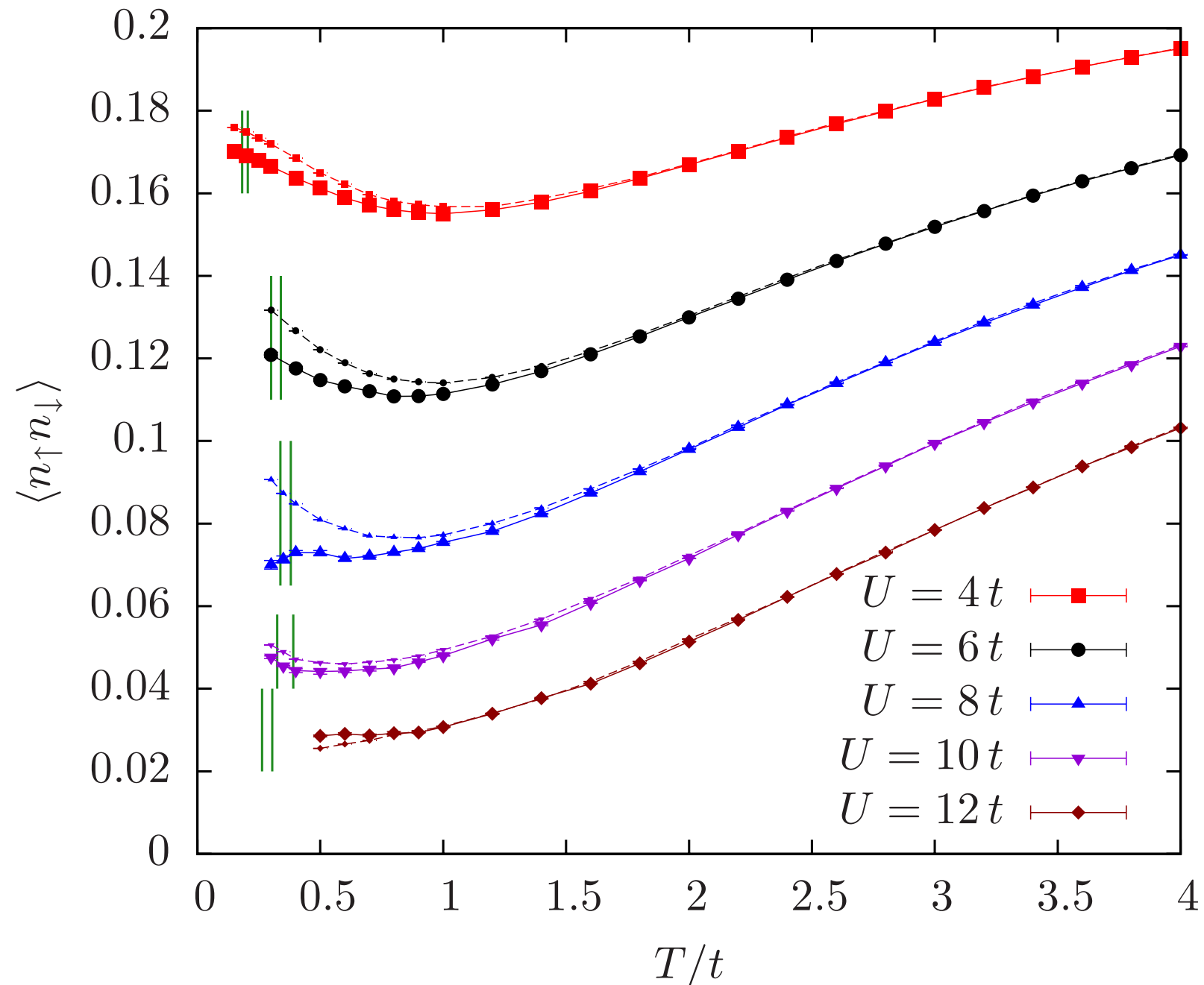
'Local' quantity shows max 20% deviations

DCA Results: The 3D Hubbard Model

Non-local quantities, e.g. nearest neighbor spin correlation function
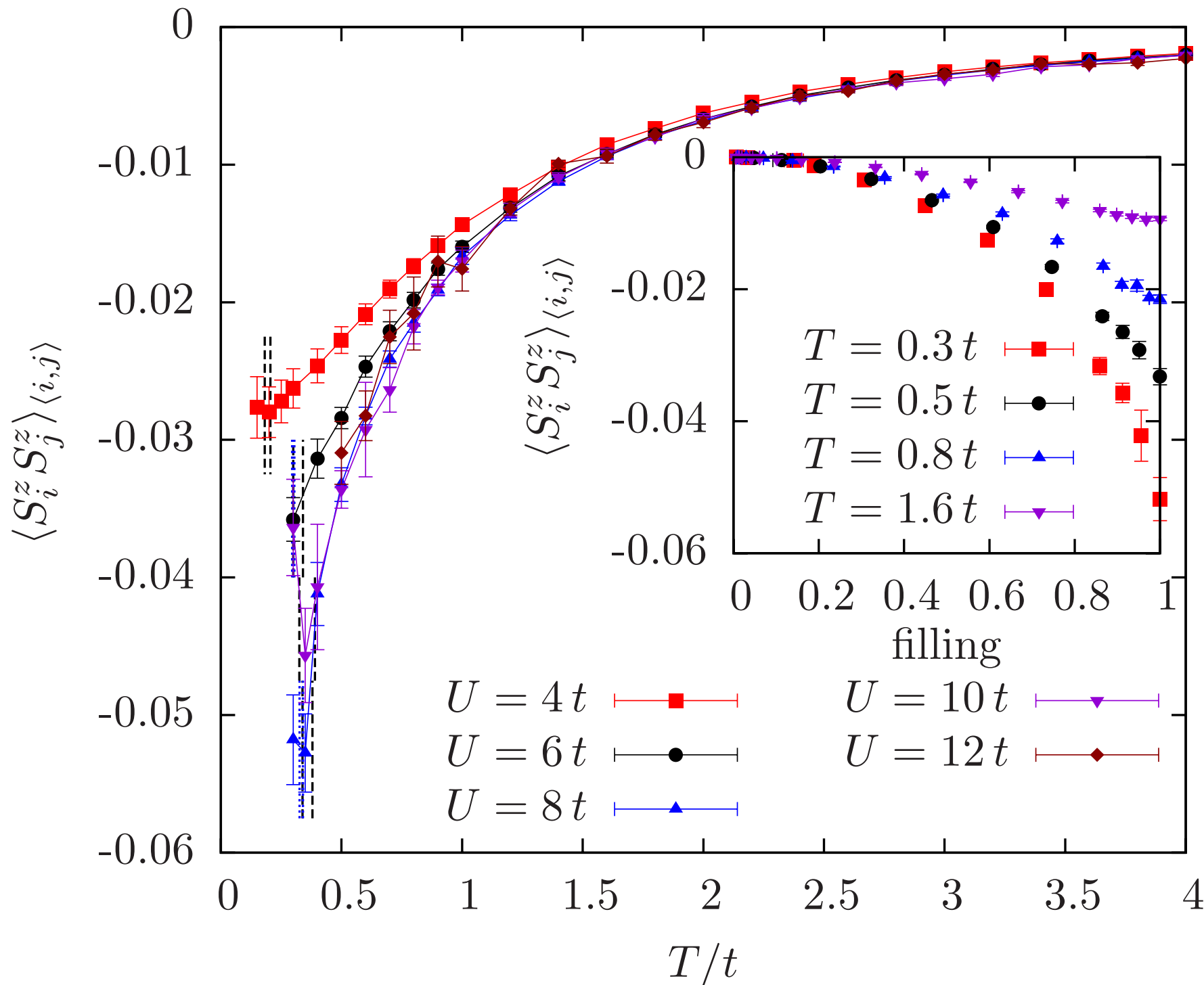
Requires cluster method, also for low filling.

Larger finite size effects.

Interesting physics: steep slope means possible candidate for thermometry; measurable in cold atom experiments.
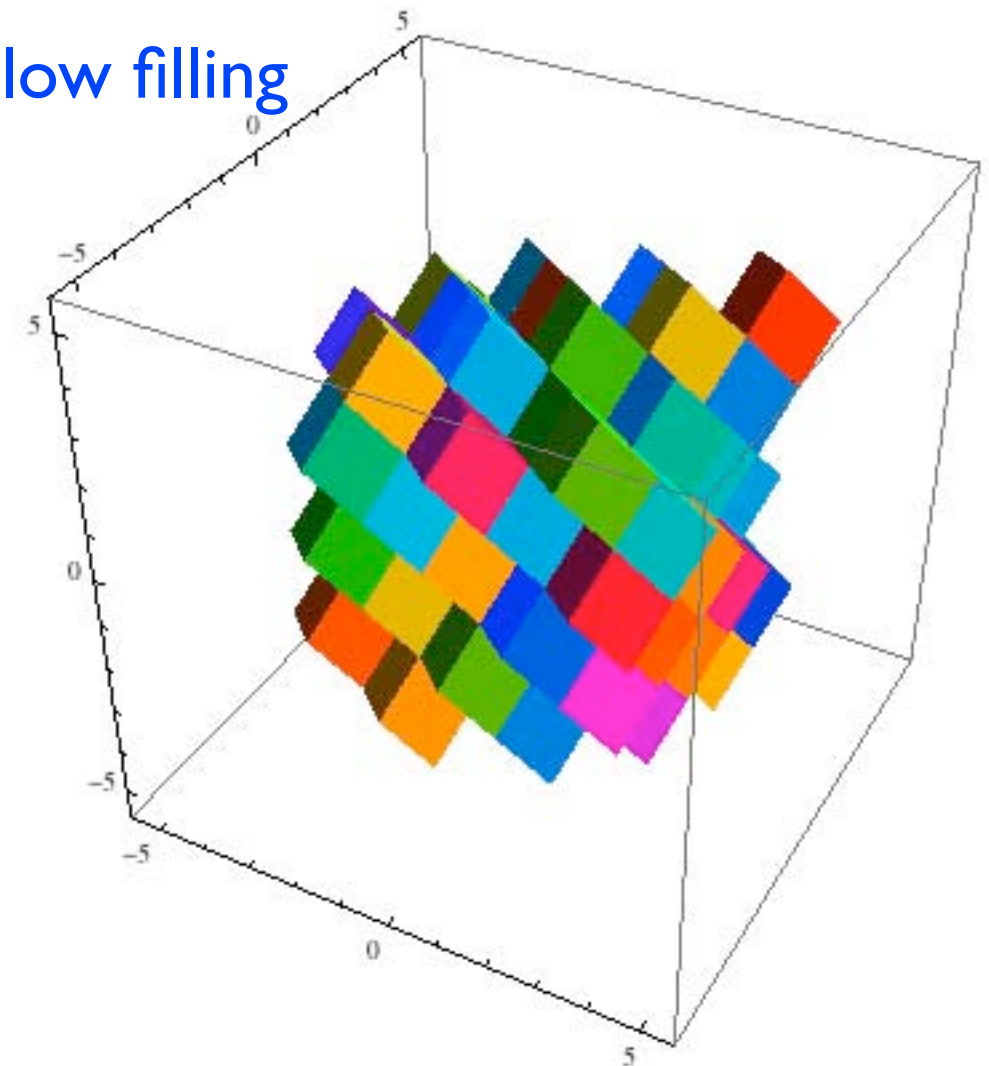
DCA Results: The 3D Hubbard Model

We have solved the 3D Hubbard model at high temperature! Full tables for the entire phase diagram with energies, densities, entropies, double occupancies, and spin correlation functions are available online

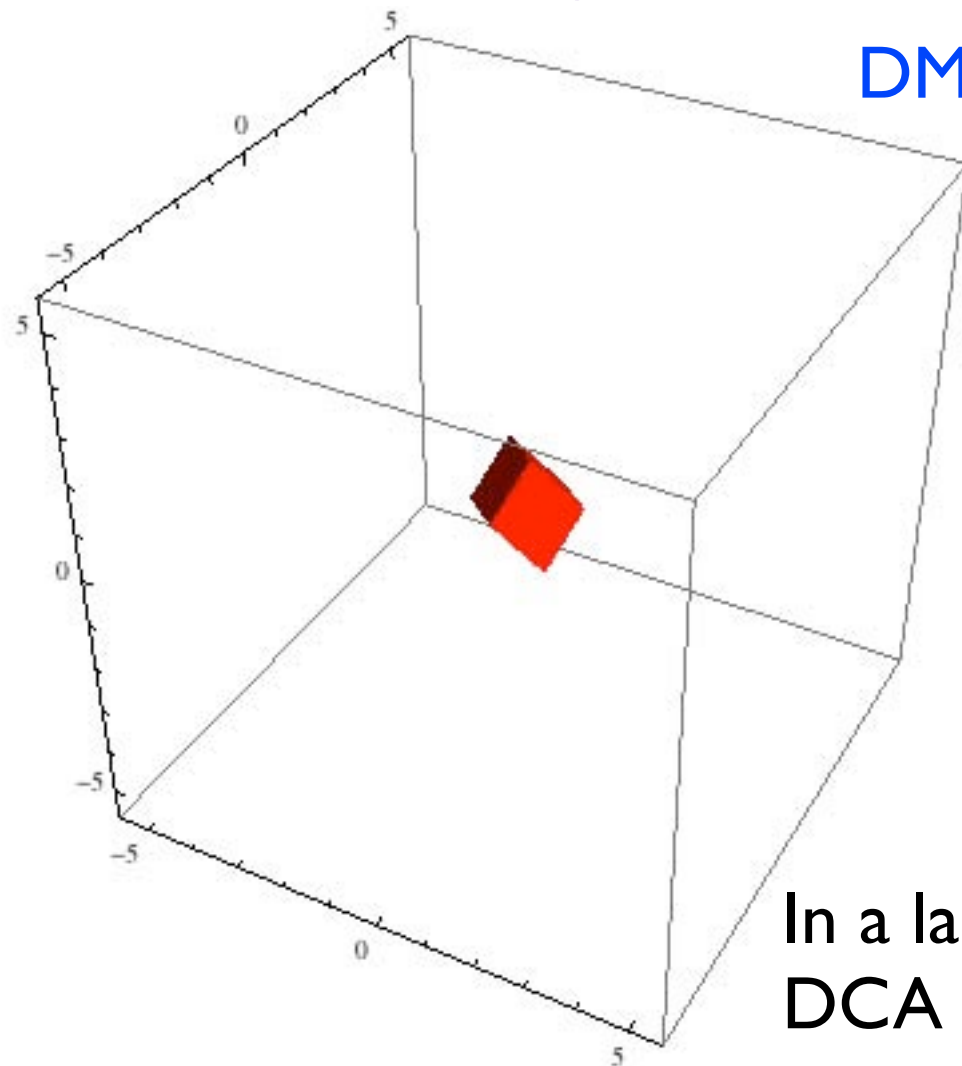[For $U \leq 12t$, and T above T_N : about 5 times lower in T than previous methods]

DCA Results: The 3D Hubbard Model
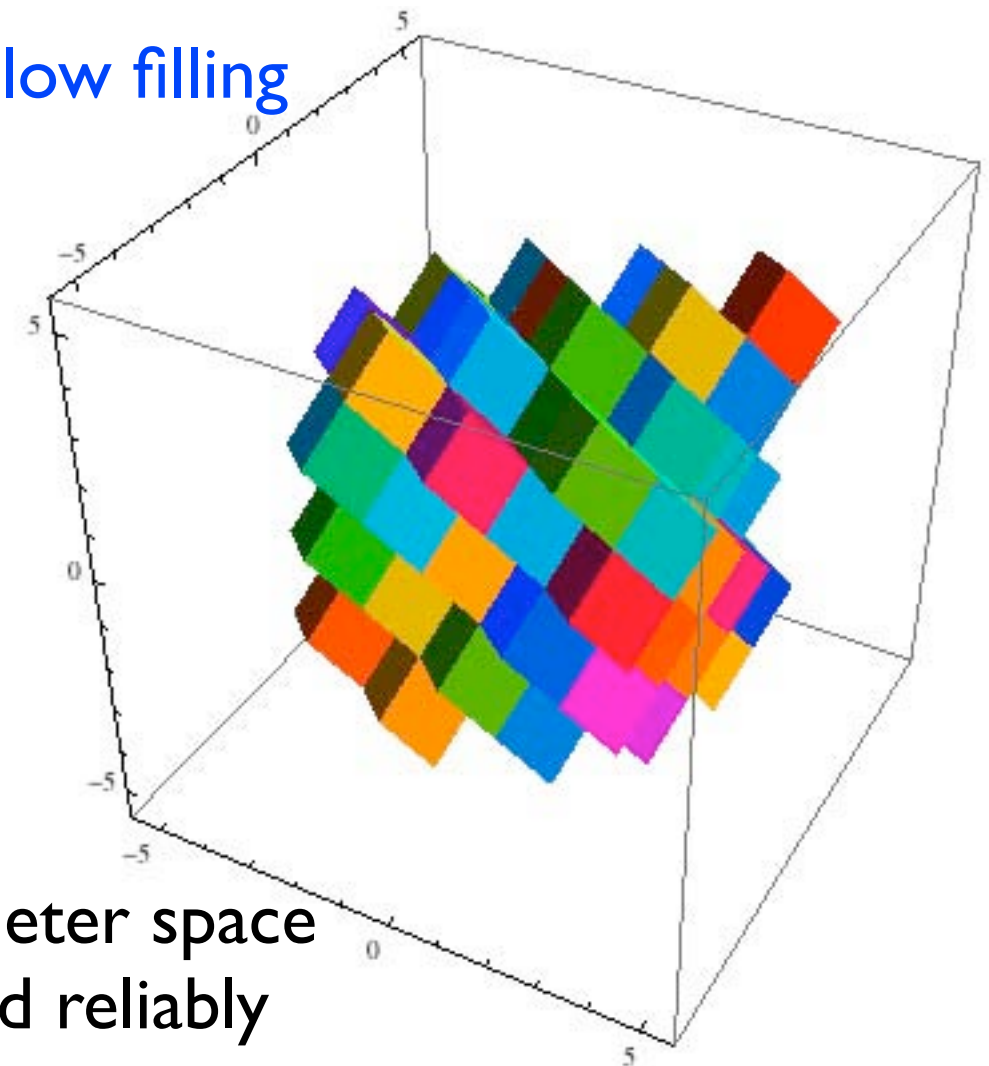
We have solved the 3D Hubbard model at high temperature! Full tables for the entire phase diagram with energies, densities, entropies, double occupancies, and spin correlation functions are available online

[For $U \leq 12t$, and T above T_N : about 5 times lower in T than previous methods]
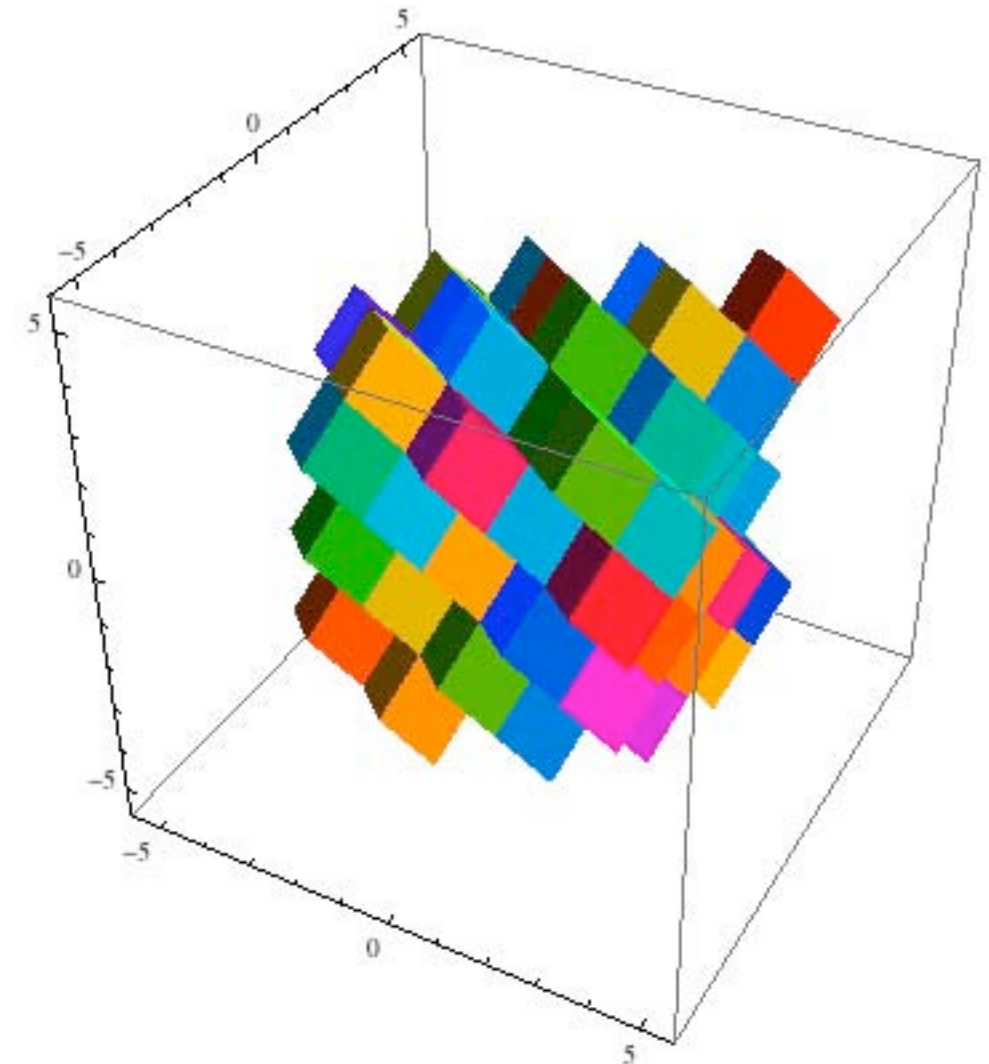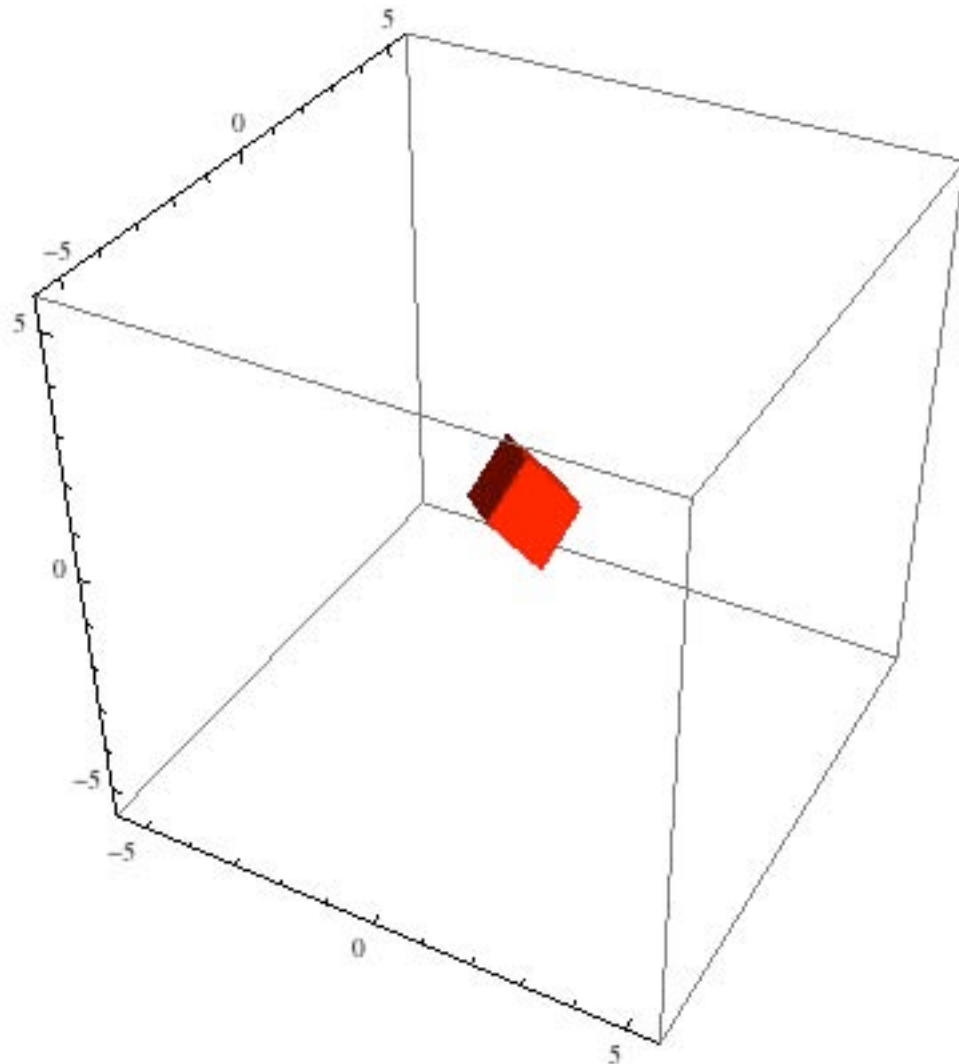
HTSE works for high T

DCA Results: The 3D Hubbard Model

We have solved the 3D Hubbard model at high temperature! Full tables for the entire phase diagram with energies, densities, entropies, double occupancies, and spin correlation functions are available online

[For $U \leq 12t$, and T above T_N : about 5 times lower in T than previous methods]

HTSE works for high T
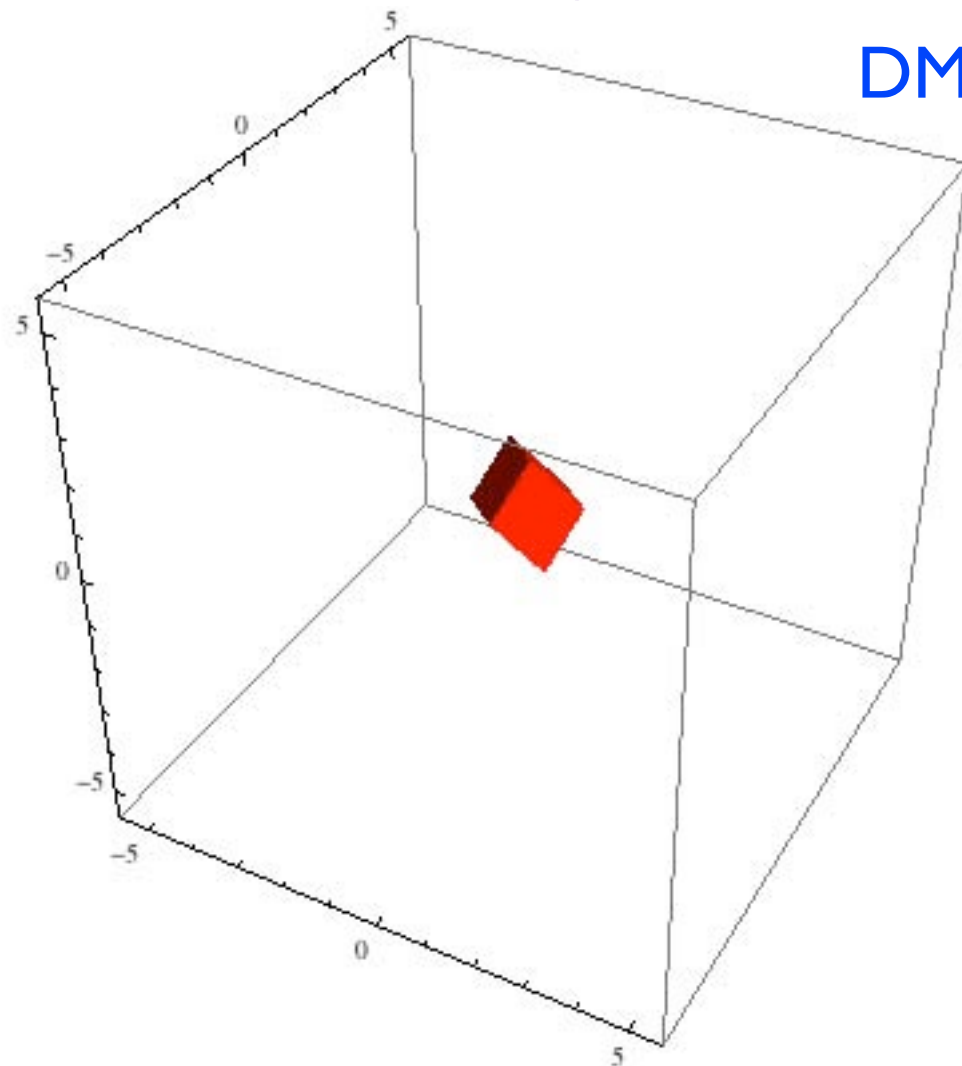
DMFT works well for low filling

DCA Results: The 3D Hubbard Model

We have solved the 3D Hubbard model at high temperature! Full tables for the entire phase diagram with energies, densities, entropies, double occupancies, and spin correlation functions are available online

[For $U \leq 12t$, and T above T_N : about 5 times lower in T than previous methods]

HTSE works for high T

DMFT works well for low filling

In a large range of parameter space DCA can be extrapolated reliably

How about 2D?

High temperature series expansion and DMFT available, similar behavior.
Convergence of cluster DMFT spot-checked for some parameters

HTSE & DMFT

U=4, half filling, 2d Hubbard model
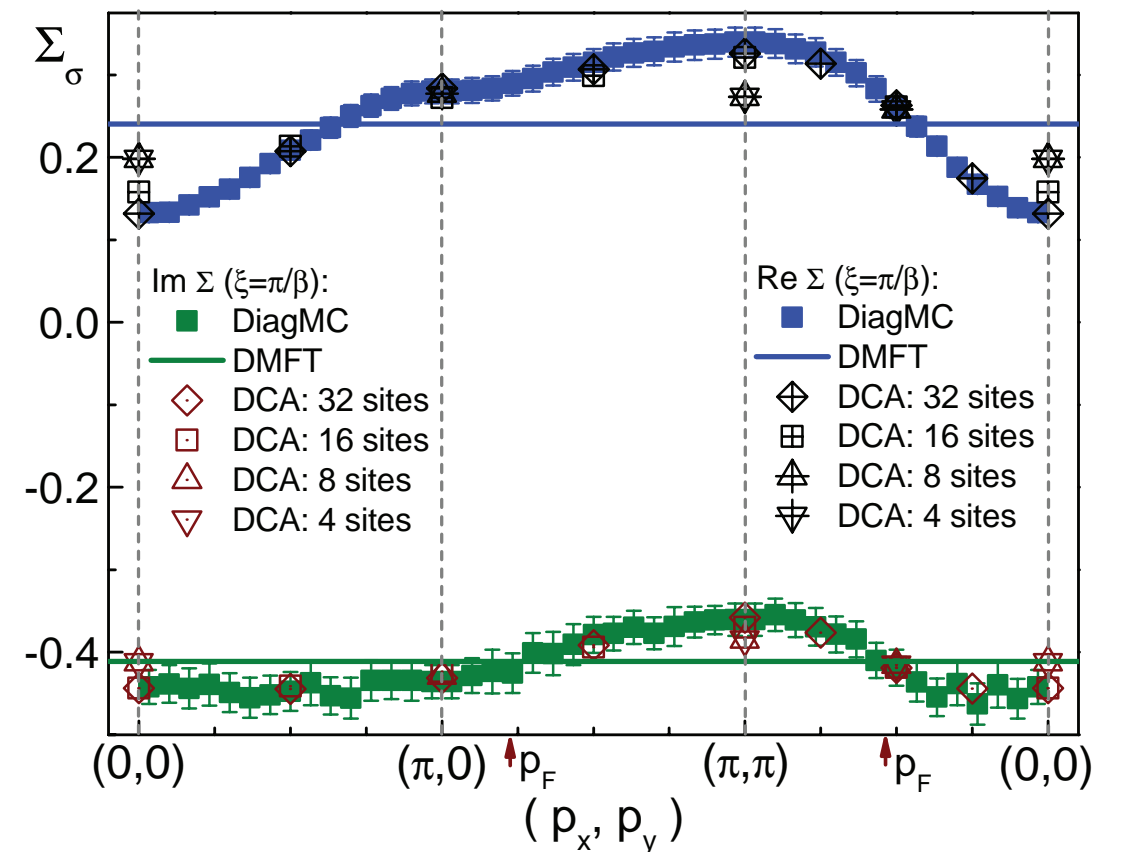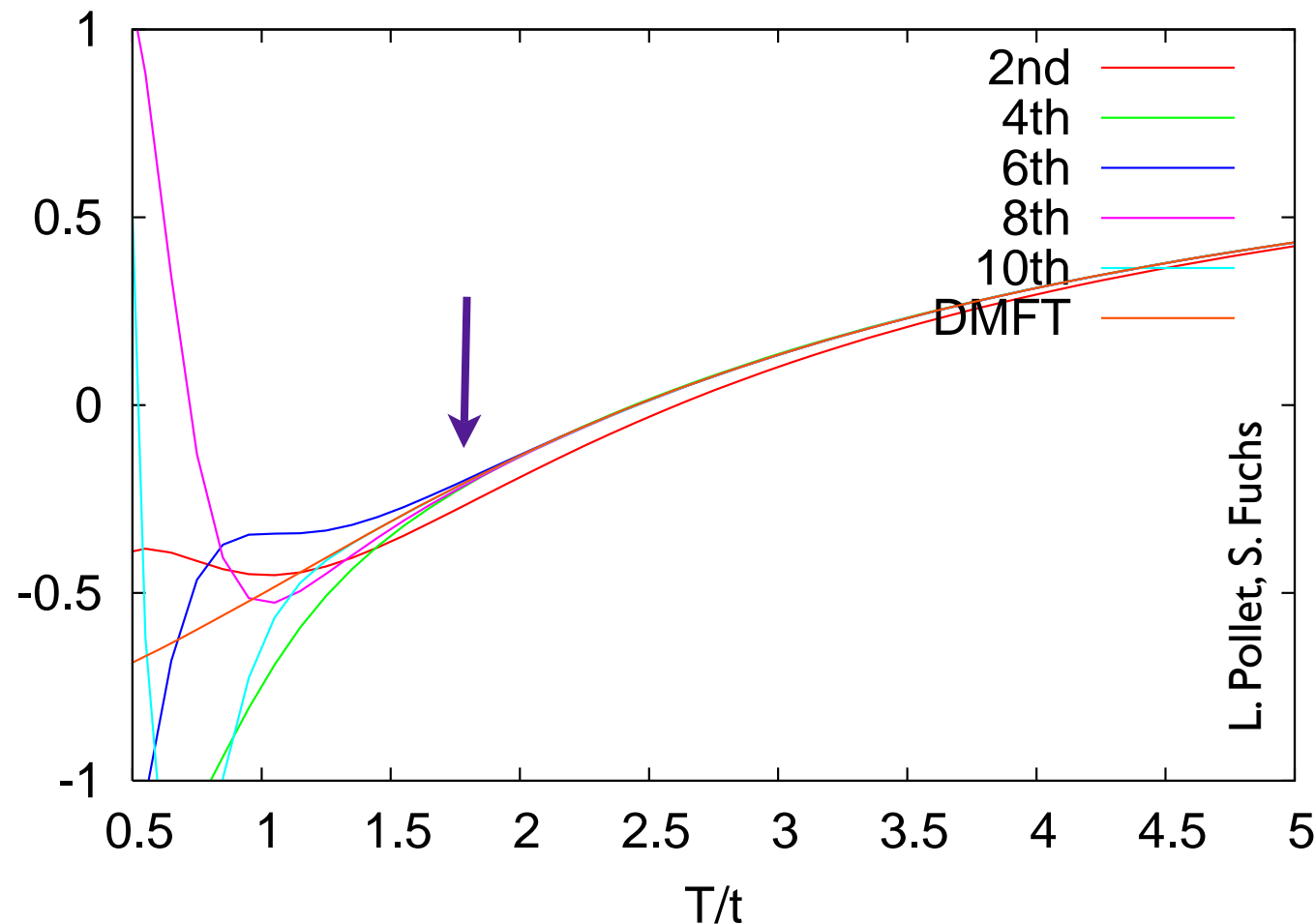
Cluster DMFT convergence vs
numerically exact DiagMC result

E. Kozik, K. van Houcke, E. Gull,
et al., EPL 90, 10004 (2010)

How about 2D?

What can we say about the interesting physics happening at much lower temperature?
Sign problem! Limit to clusters of size ≤16 for surveys of the entire phase space
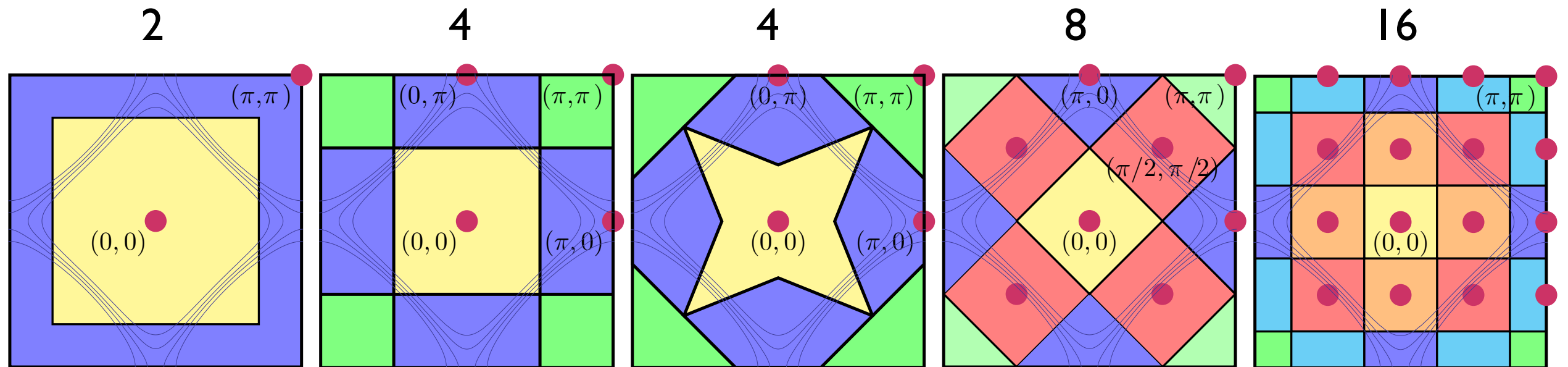
Qualitative answers, not quantitative extrapolations: Which results are cluster specific, which are universal? How do results change by going to larger and larger clusters? Which parts of the phase diagram are converged?

Previous / Other work on (mostly small) cluster DMFT in 2D:

O. Parcollet, G. Biroli, and G. Kotliar, Phys. Rev. Lett. 92, 226402 (2004), M. Civelli, M. Capone, S. S. Kancharla, O. Parcollet, and G. Kotliar, Phys. Rev. Lett. 95, 106402 (2005), T. Maier, M. Jarrell, T.C. Schulthess, P.R.C. Kent, J.B. White, Phys. Rev. Lett. 95, 237001 (2005), B. Kyung, S. S. Kancharla, D. Sénéchal, A.-M. S. Tremblay, M. Civelli, and G. Kotliar, Phys. Rev. B 73, 165114 (2006), T. D. Stanescu and G. Kotliar, Phys. Rev. B 74, 125110 (2006), A. Macridin, M. Jarrell, T. Maier, P. R. C. Kent, and E. D'Azevedo, Phys. Rev. Lett. 97, 036401 (2006), Y. Z. Zhang and M. Imada, Phys. Rev. B 76, 045108 (2007), M. Civelli, M. Capone, A. Georges, K. Haule, O. Parcollet, T. D. Stanescu, and G. Kotliar, Phys. Rev. Lett. 100, 046402 (2008), E. Gull, P. Werner, X. Wang, M. Troyer, and A. J. Millis, EPL 84, 37009 (2008), H. Park, K. Haule, and G. Kotliar, Phys. Rev. Lett. 101, 186403 (2008), M. Ferrero, P. S. Cornaglia, L. D. Leo, O. Parcollet, G. Kotliar, and A. Georges, EPL 85, 57009 (2009), M. Ferrero, P. S. Cornaglia, L. De Leo, O. Parcollet, G. Kotliar, and A. Georges, Phys. Rev. B 80, 064501 (2009), M. Civelli, Phys. Rev. B 79, 195113 (2009), A. Liebsch and N.-H. Tong, Phys. Rev. B 80, 165126 (2009), N. Lin, E. Gull, and A. J. Millis, Phys. Rev. B 80, 161105(R) (2009), S. Sakai, Y. Motome, and M. Imada, Phys. Rev. Lett. 102, 056404 (2009), G. Sordi, K. Haule, and A. Tremblay, Phys. Rev. Lett. 104, 226402 (2010), S. Sakai, Y. Motome, and M. Imada, arXiv:1004.2569, M. Ferrero, O. Parcollet, G. Kotliar, and A. Georges, arXiv:1001.5051.
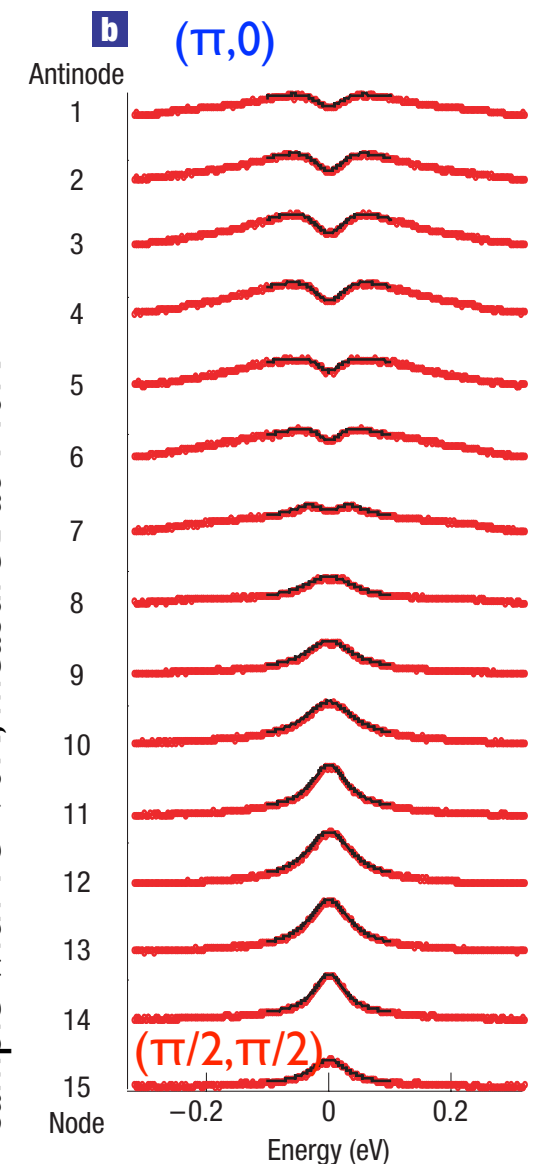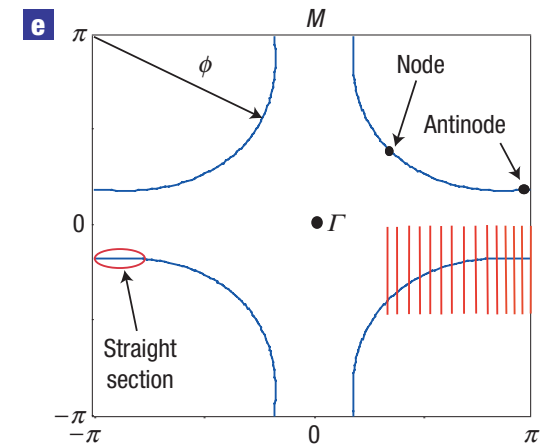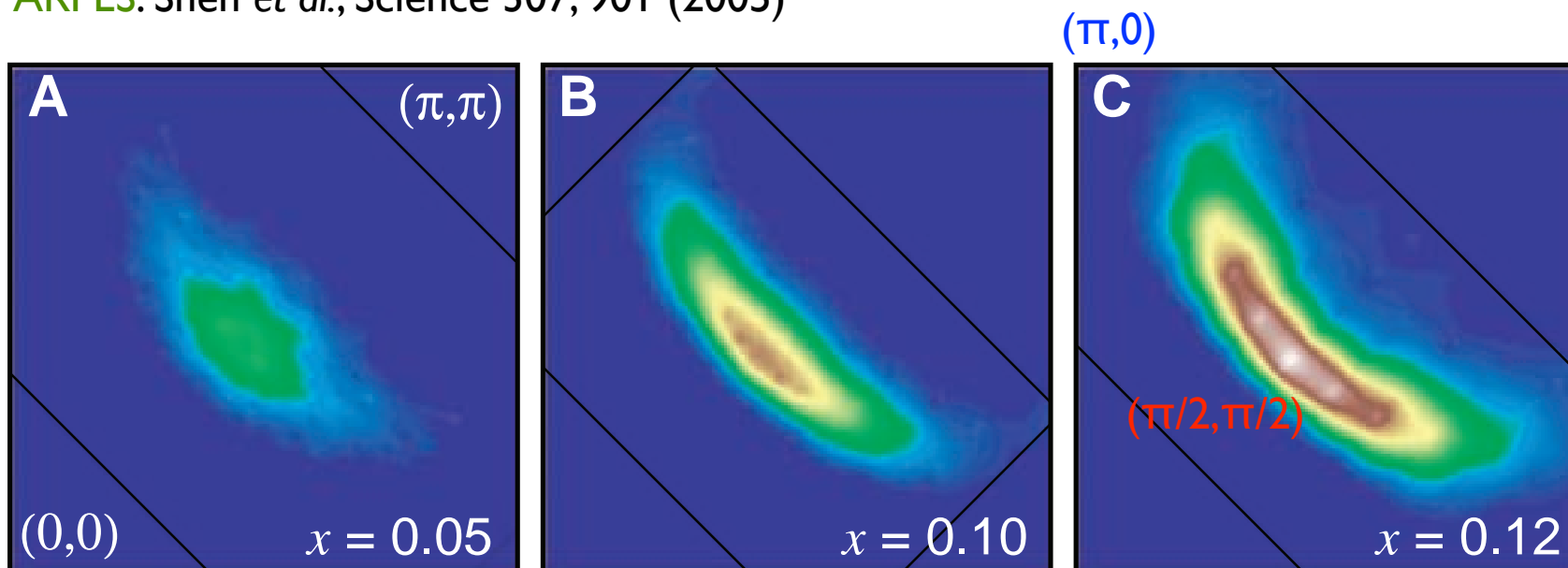
Motivation - Pseudogap

in high-Tc materials: Electronic spectral function is suppressed along the BZ face, but not along zone diagonal.

No (obvious) long range order.

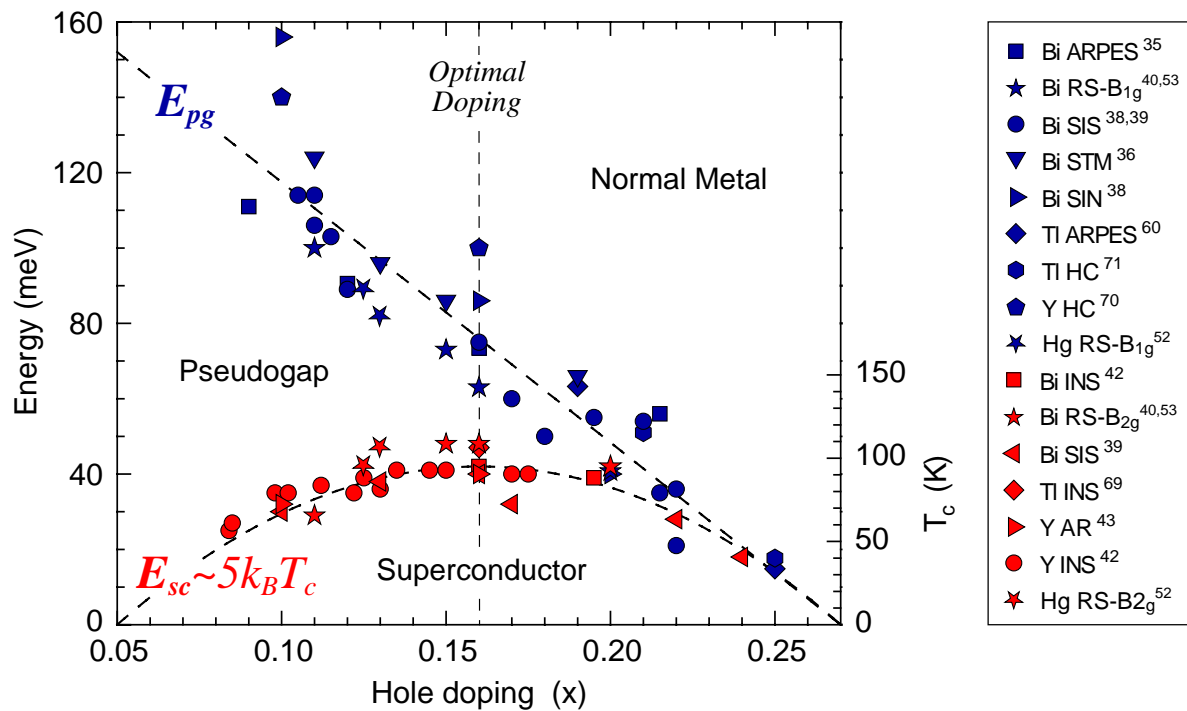Key physics dependence on momentum around Fermi surface, Difference of spectral function around Fermi surface.

Controversial if contained in Hubbard model without long ranged order.

ARPES: Shen *et al.*, Science 307, 901 (2005)

ARPES: Kanigel et al., Nature Physics 2, 447 - 451 (2006). Bi2212 sample with Tc=90K, measured at 140K

Motivation - Pseudogap

Property of underdoped cuprates

Hüfner *et al.*, Rep. Prog. Phys. 71, 062501(2008)

Observed in various experimental probes

cyan: T > Tc

Homes et al., Phys. Rev. Lett. 71, 1647 (1993). c-axis conductivity, Tc=63K
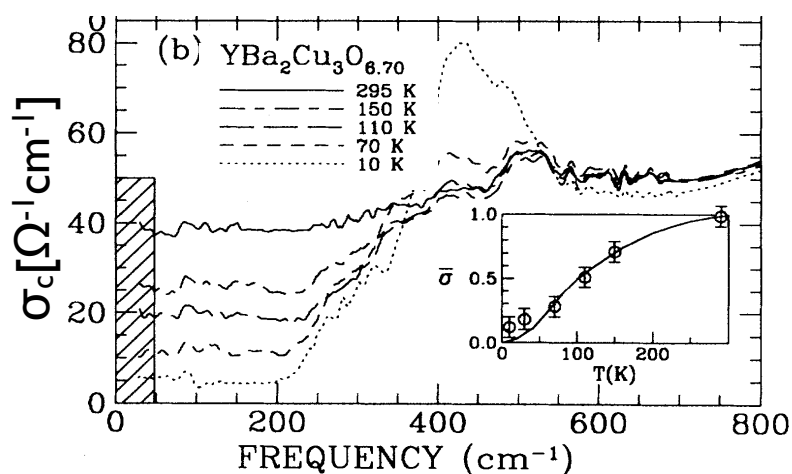
Renner *et al.*, Phys. Rev. Lett. 80, 149 (1998). Tunneling spectra of Bi2212 sample with Tc=83K
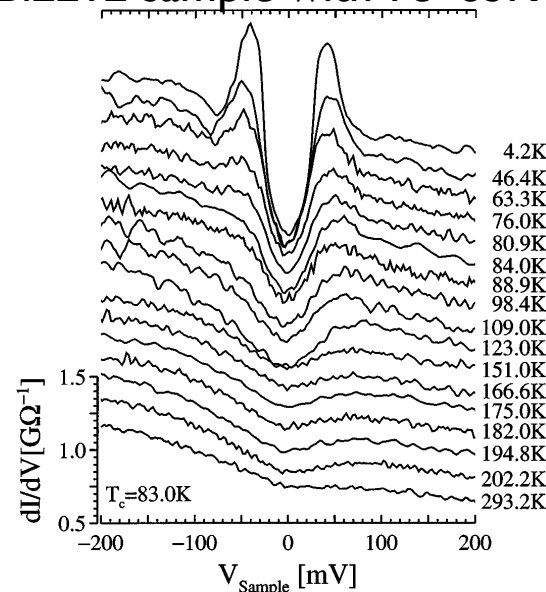
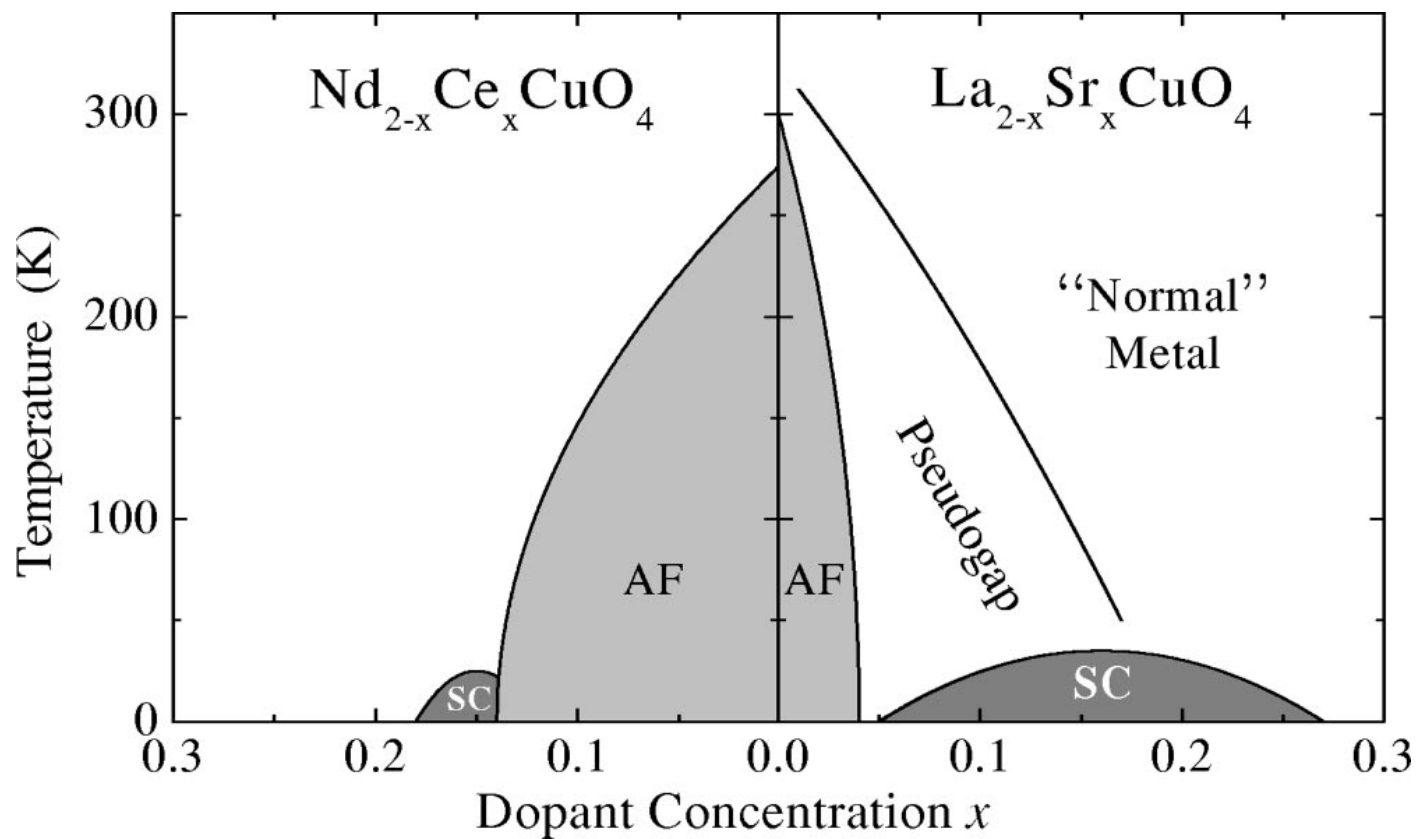S. Blanc *et al.*, unpublished: Raman spectroscopy on $HgBa_2CuO_{4+\delta}$
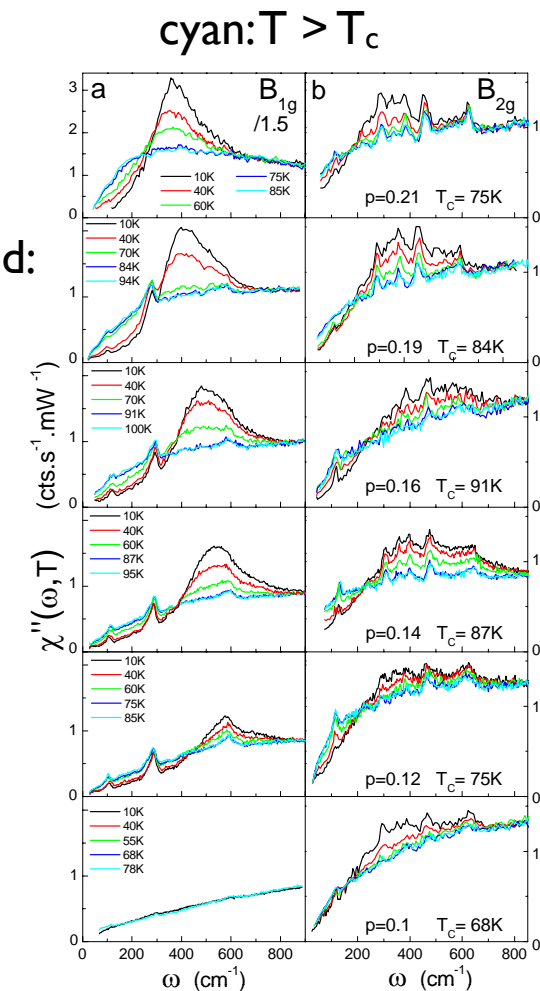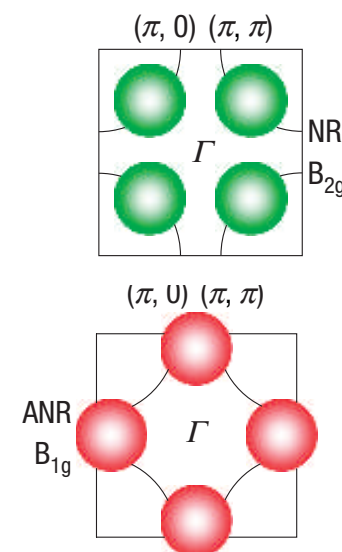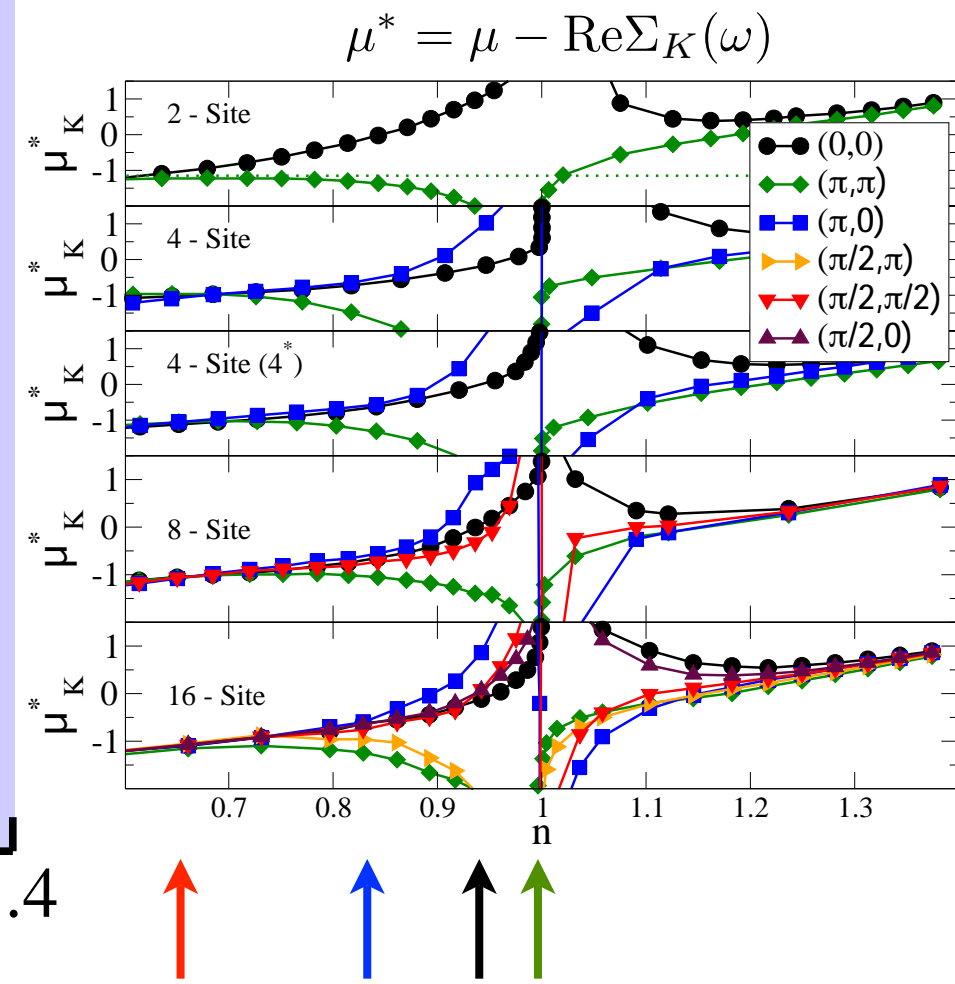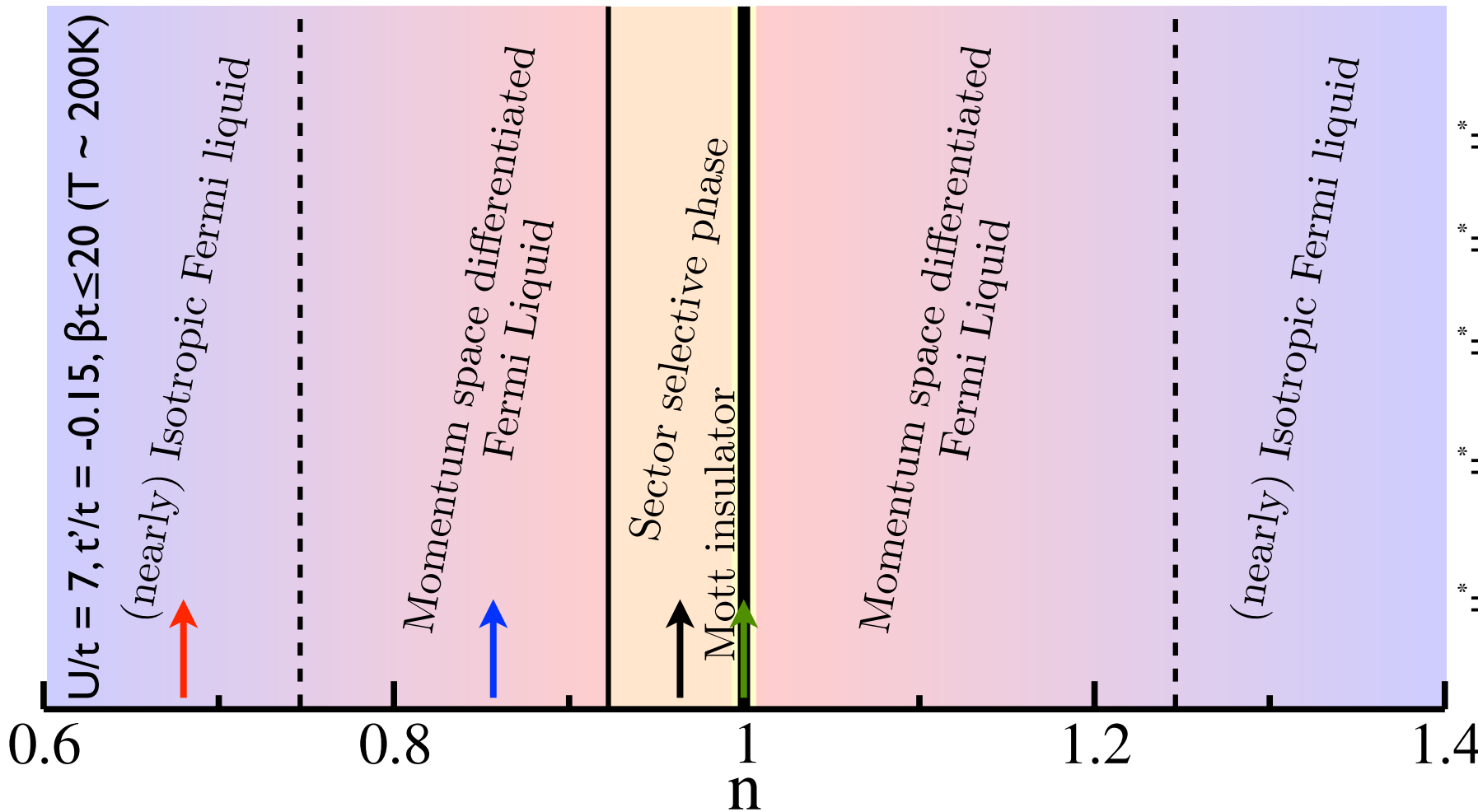
Difference of electron and hole doping

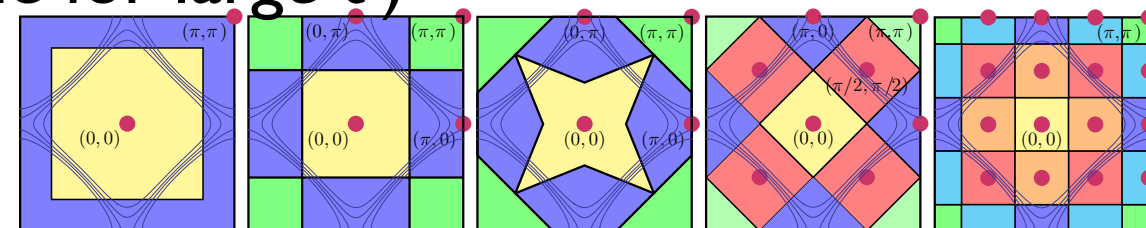Damascelli *et al.*, Rev. Mod. Phys 75, 2 (2003)

FIG. 1. Phase diagram of *n*- and *p*-type superconductors, showing superconductivity (SC), antiferromagnetic (AF), pseudogap, and normal-metal regions.

Pseudogap appears only on the hole doped side (right side),

dopings smaller than optimal doping,

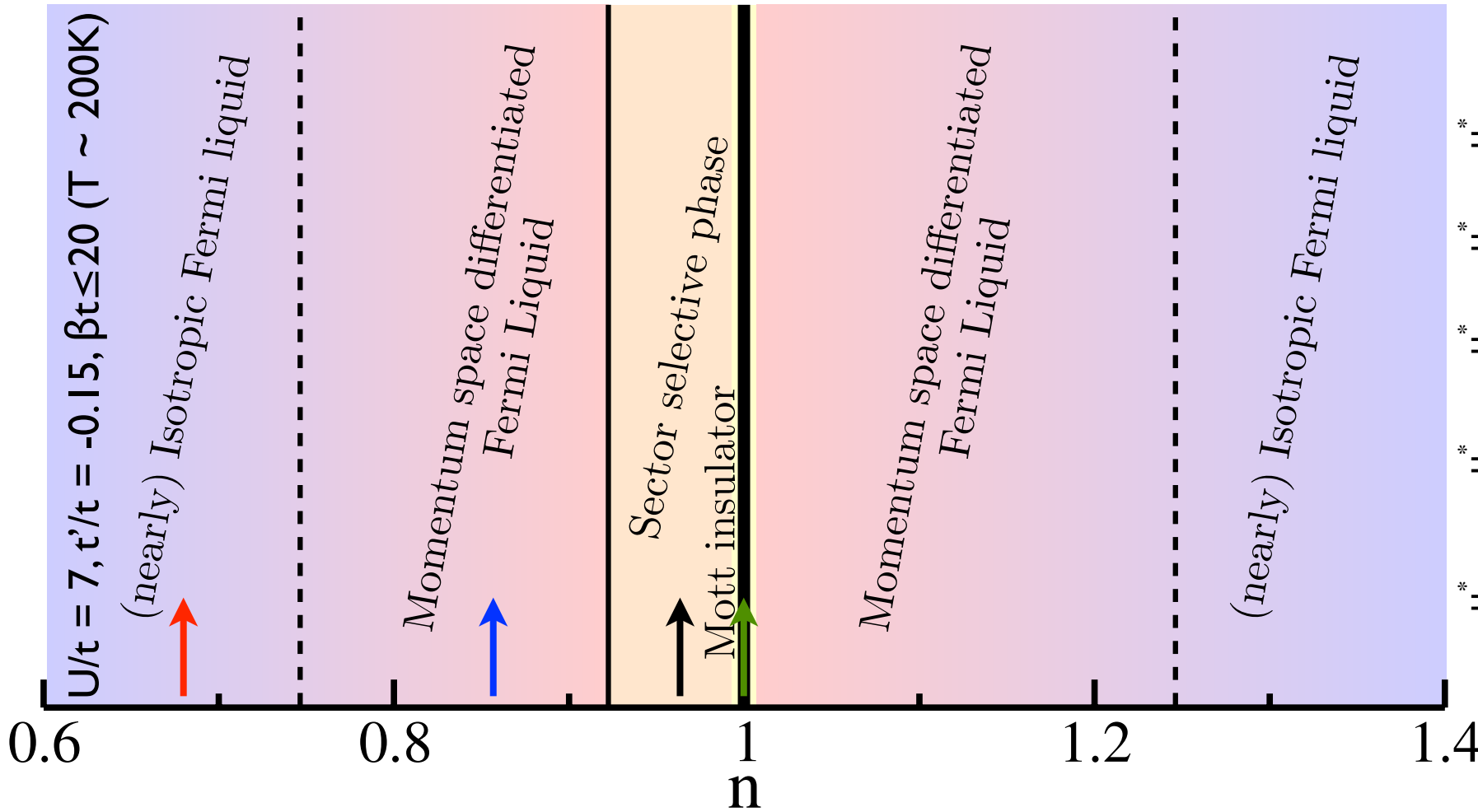Temperatures up to ~ 300K

Results: Regimes – Doping


Study on five cluster geometries shows same features:

- Isotropic Fermi Liquid for large doping, as in 3D $\Sigma(k,\omega) = \Sigma(\omega)$

- Momentum space differentiated Fermi liquid regime

- Sector Selective Phase (absent on el-doped side for large t')

- Mott Insulator

Results: Regimes – Doping
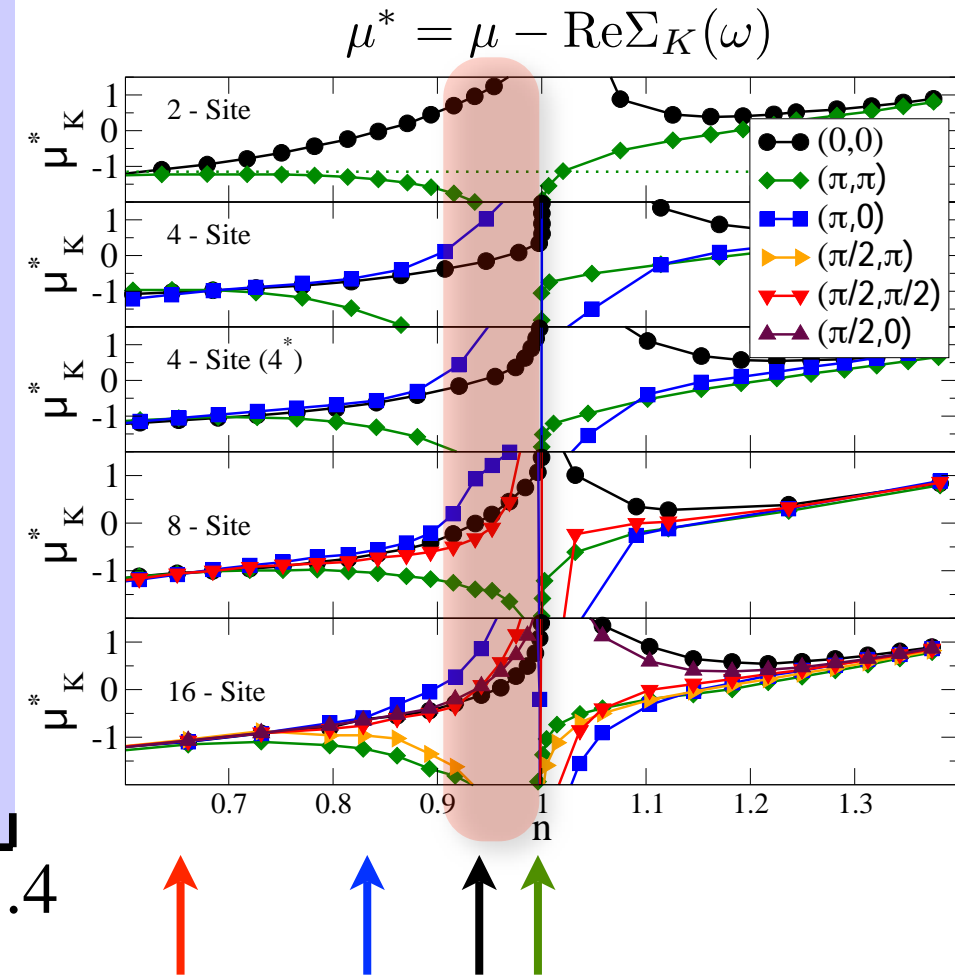
$$\mu^* = \mu - \mathrm{Re}\Sigma_K(\omega)$$

Study on five cluster geometries shows same features:

- Isotropic Fermi Liquid for large doping, as in 3D $\Sigma(k,\omega) = \Sigma(\omega)$

- Momentum space differentiated Fermi liquid regime

- Sector Selective Phase (absent on el-doped side for large t')

- Mott Insulator
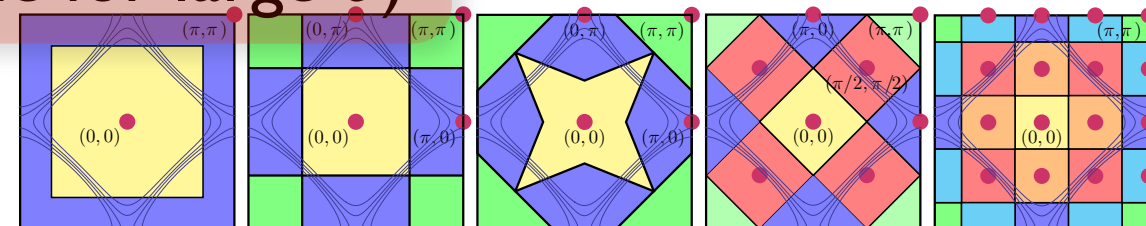
Results: Sector Selective Regime

Sector selectivity:

- Some momentum sectors become insulating, while others stay metallic.

- Region around (π,0) insulating, quasiparticles in (π/2,π/2) region.
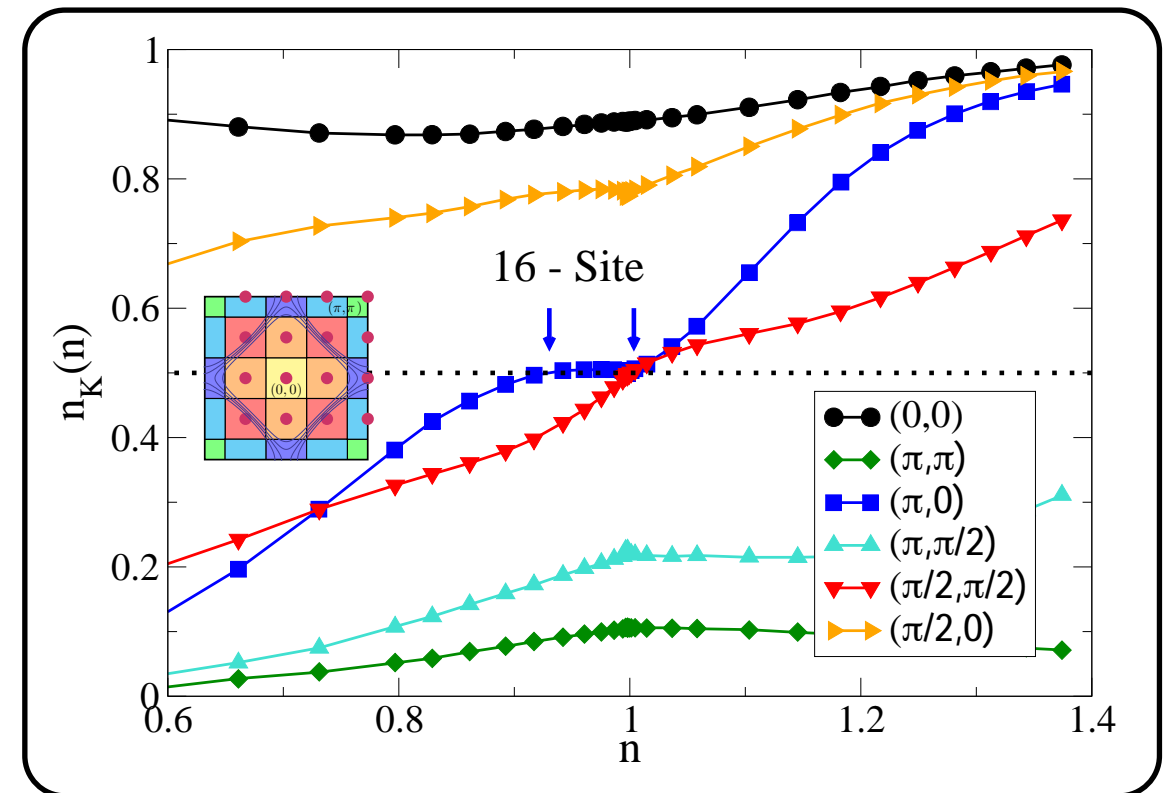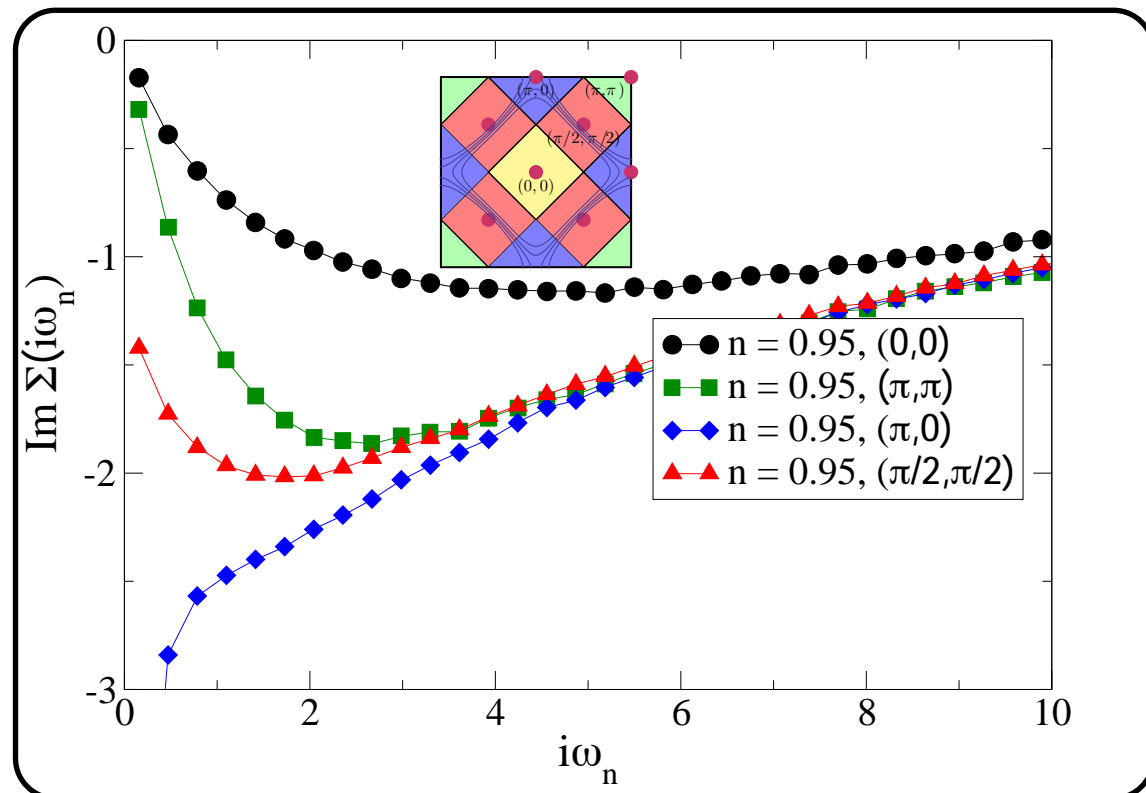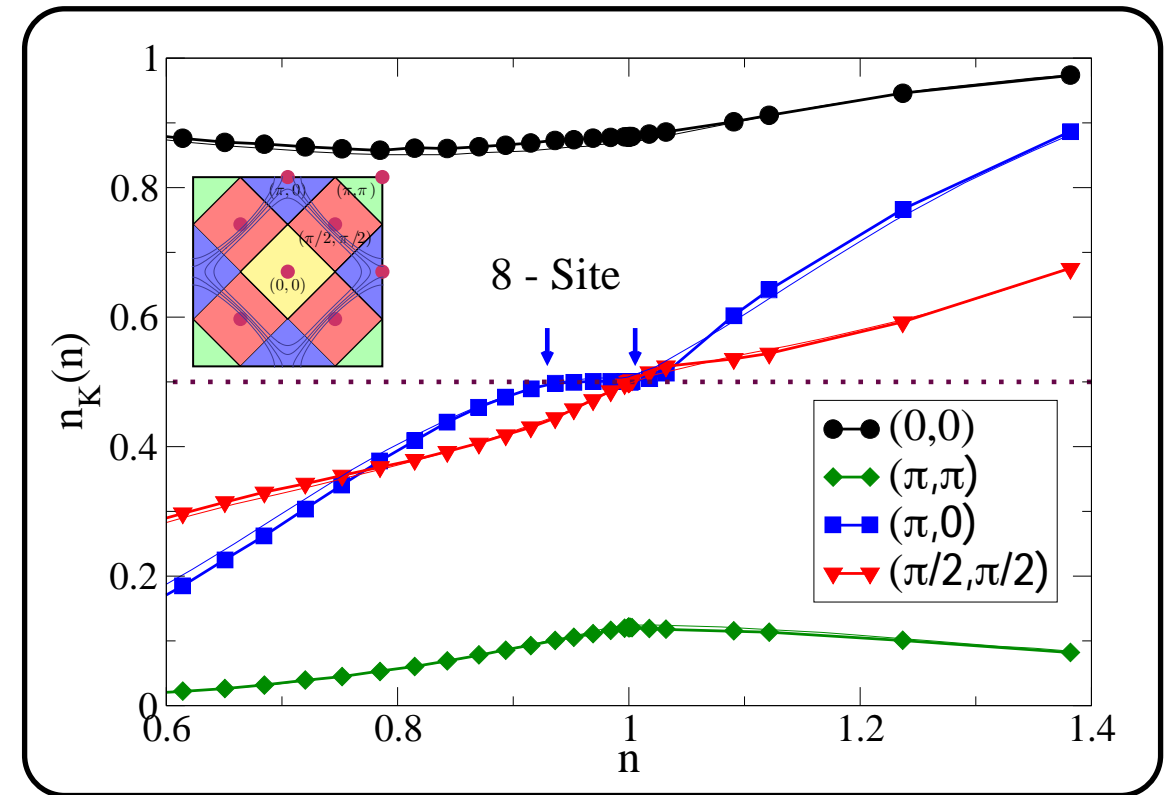
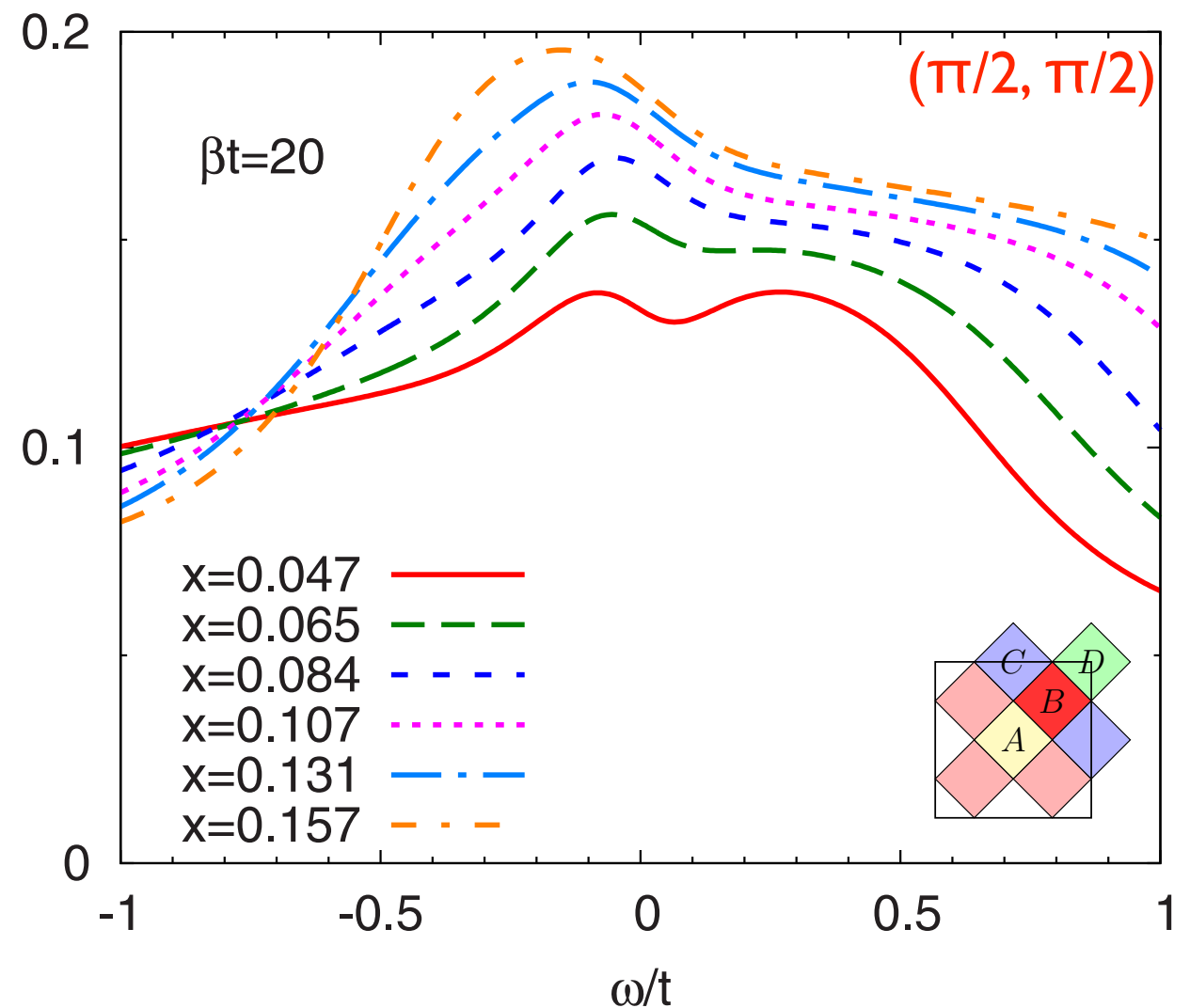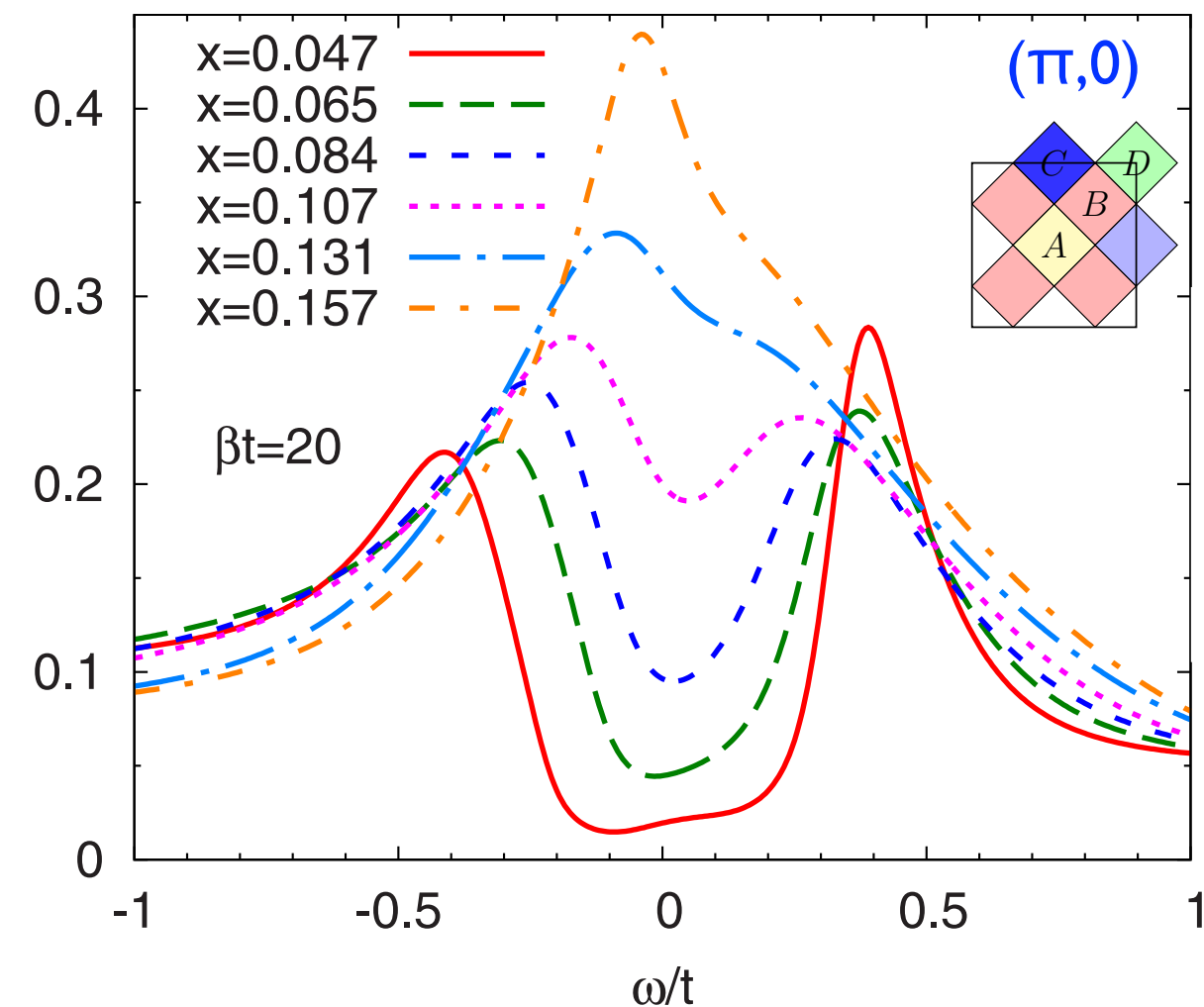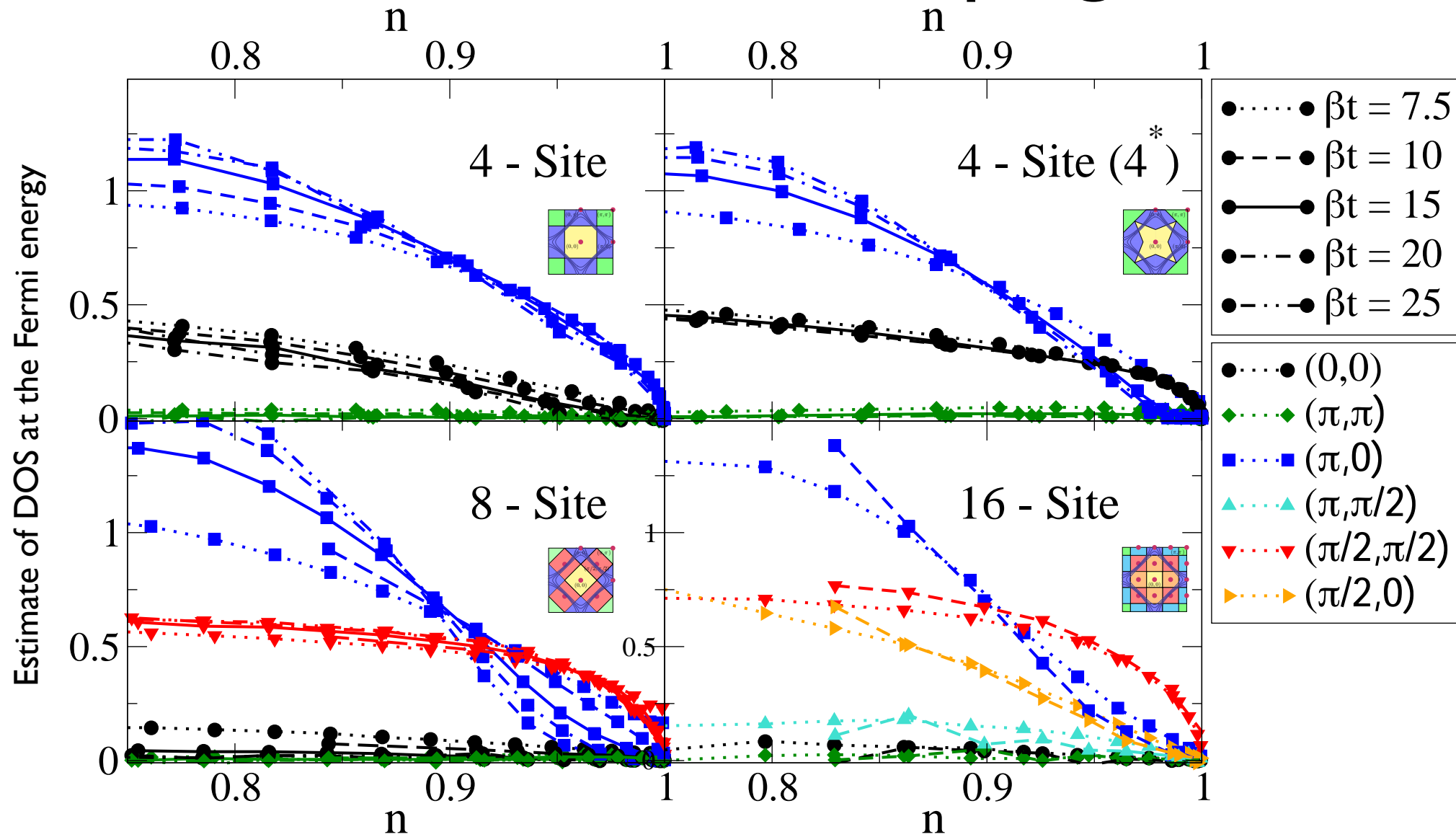# Results: Spectral Function

Analytic continuations
by Nan Lin

Analytically continued spectral function A(ω) for the
antinodal and the nodal sector, as a function of doping x

(π,0)

x=0.047
x=0.065
x=0.084
x=0.107
x=0.131
x=0.157

βt=20

ω/t

(π/2, π/2)

βt=20

x=0.047
x=0.065
x=0.084
x=0.107
x=0.131
x=0.157

ω/t   Ω/t
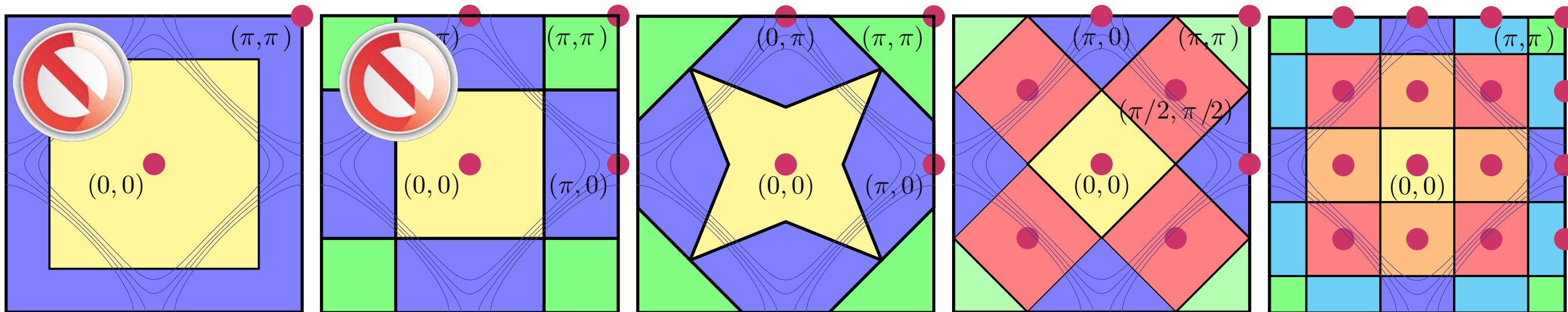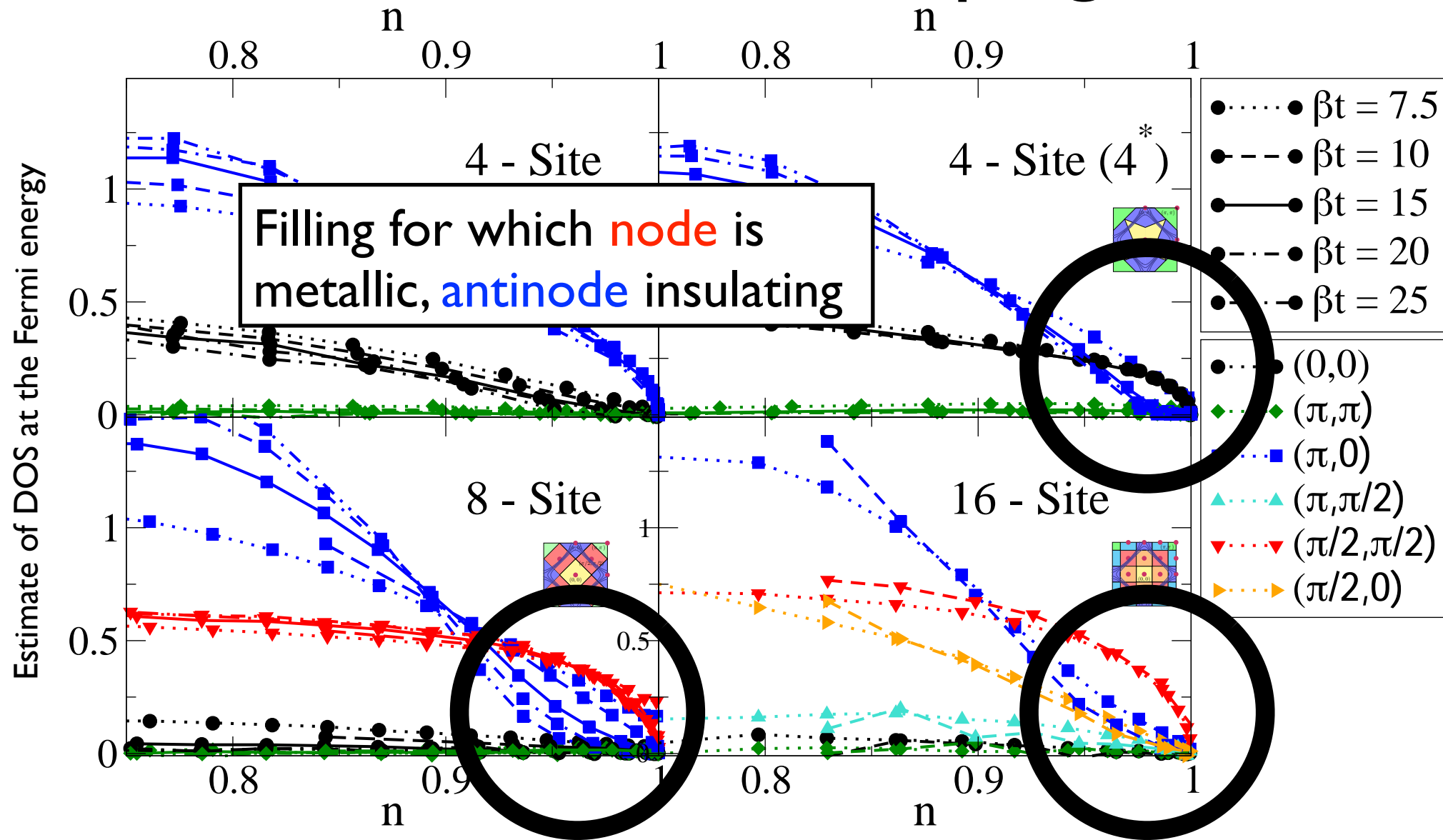
U = 7t, t'/t=0.15, βt=20

Results: Doping Transition

Sector selective transition is robust in DCA (for all clusters large enough to have nodal antinodal differentiation), is the DCA representation of pseudogap physics.

Results: Doping Transition

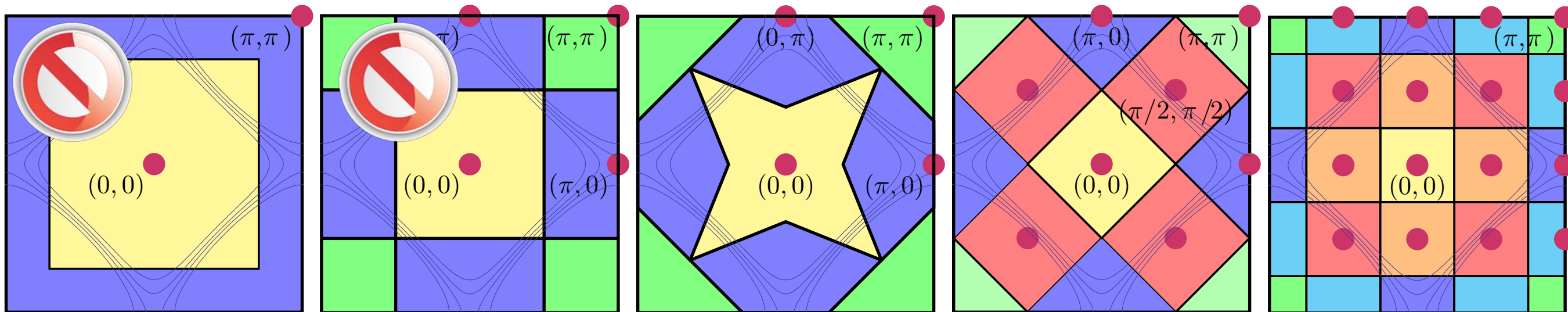Filling for which node is metallic, antinode insulating

Sector selective transition is robust in DCA (for all clusters large enough to have nodal antinodal differentiation), is the DCA representation of pseudogap physics.
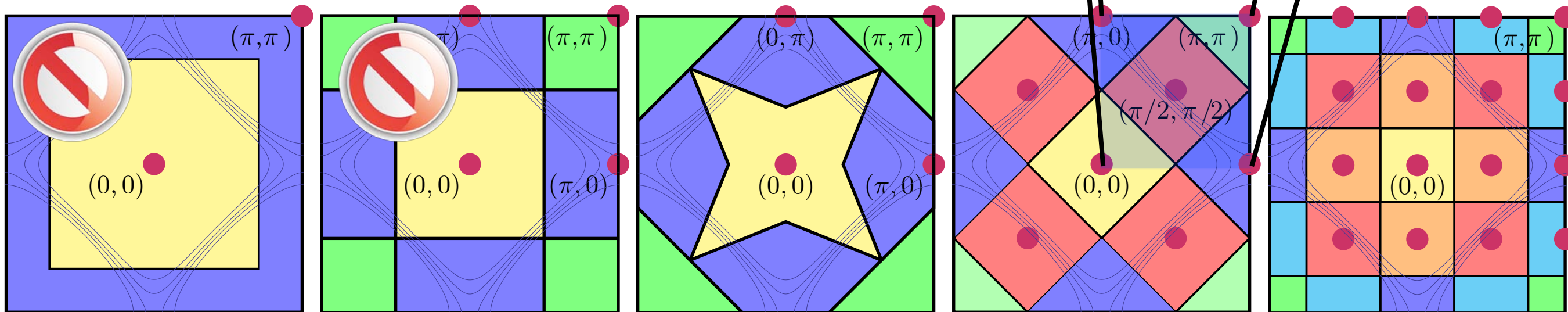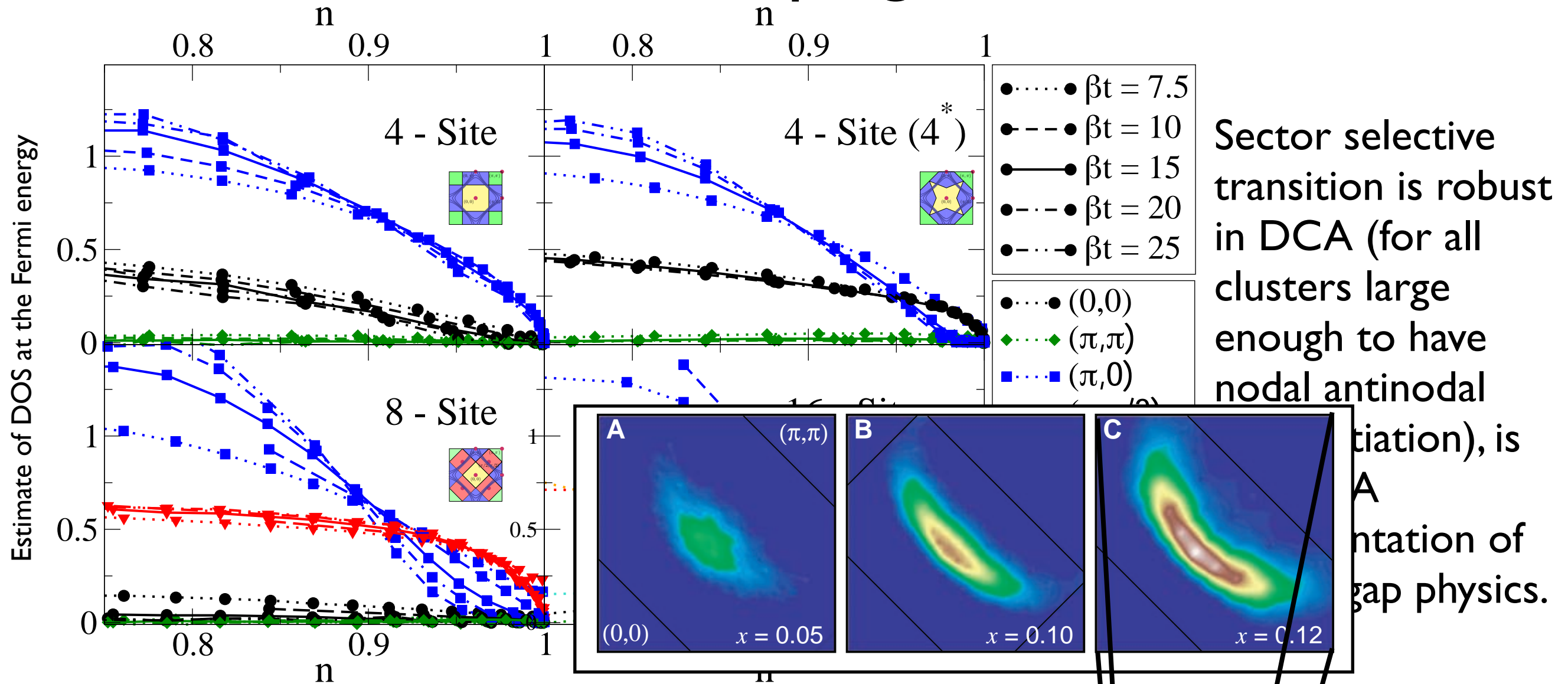
$\beta t = 7.5$
$\beta t = 10$
$\beta t = 15$
$\beta t = 20$
$\beta t = 25$

$(0,0)$
(π,π)
$(\pi,0)$
$(\pi,\pi/2)$
$(\pi/2,\pi/2)$
$(\pi/2,0)$

4 - Site

4 - Site (4^*)

8 - Site

16 - Site

Results: Doping Transition

Sector selective transition is robust in DCA (for all clusters large enough to have nodal antinodal differentiation), is ... A ... ntation of ... gap physics.

Results: Pseudogap Phase

Sector selective transition is robust (for all clusters large enough to have nodal antinodal differentiation), is the cluster DMFT representation of pseudogap physics.
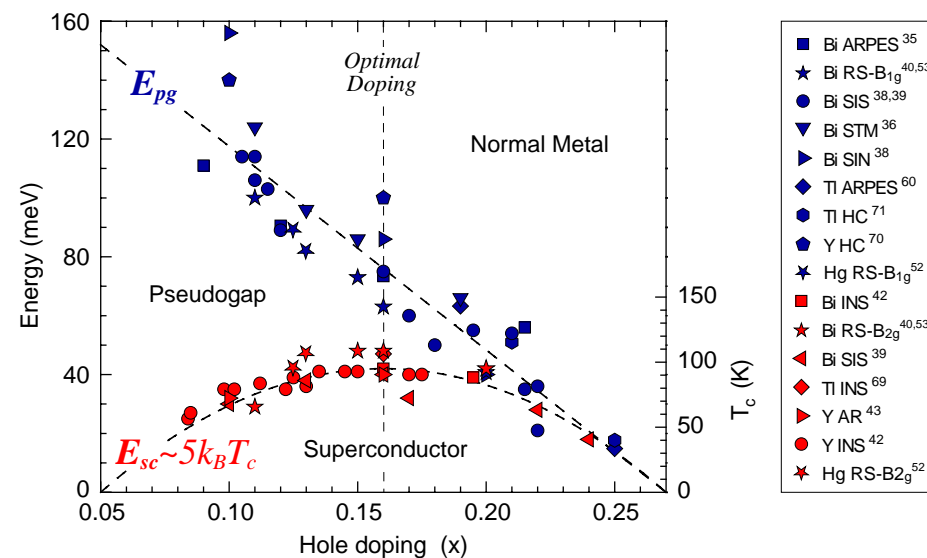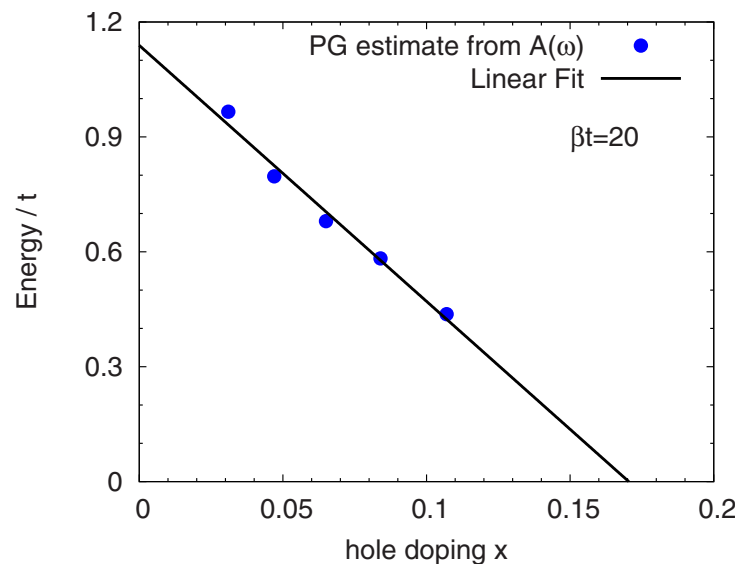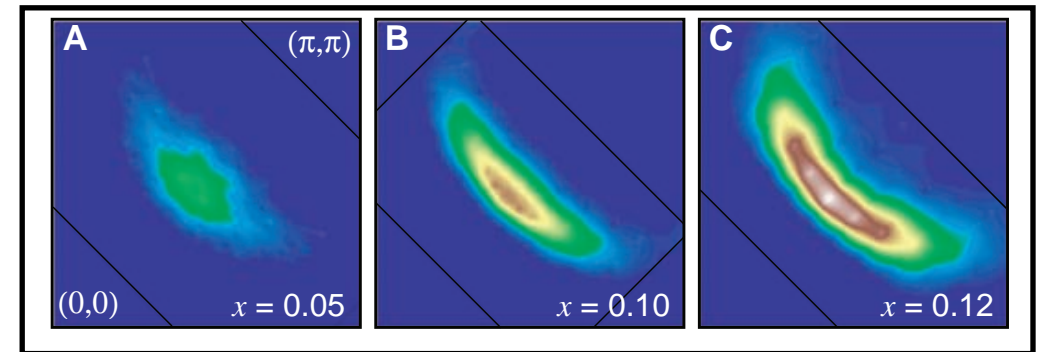

Pseudogap Size

FIG. 15. (Color online) Points: pseudogap size determined from electron spectral function as a function of hole doping x for $U=7t$ and inverse temperature $\beta=20/t \approx 200$ K. Line: linear fit to results.

Hüfner *et al.*, Rep. Prog. Phys. 71, 062501 (2008)

The pseudogap is a feature of the Hubbard model at intermediate correlation strength. No long range order is required to obtain a pseudogap.

Remarkable agreement with other experimental probes: c-axis, in-plane optical conductivity, Raman.

N. Lin, E. Gull, and A.J. Millis, Phys. Rev. B 82, 045104 (2010)

Large Cluster DMFT – Conclusions

We can do large interacting systems (100 sites and more), at and away from half filling

To obtain converged results all sources of errors need be addressed:

- Monte Carlo errors

- Finite size errors

- In methods that have them: further internal systematic errors like Trotter errors or bath discretization errors

In 3D: Exact results for temperatures five times lower

In 2D: Features in phase diagram established as robust, clear which regimes are converged and which are not.

Progress made possible by advances in numerical methods: CT-AUX and sub-matrix updates.
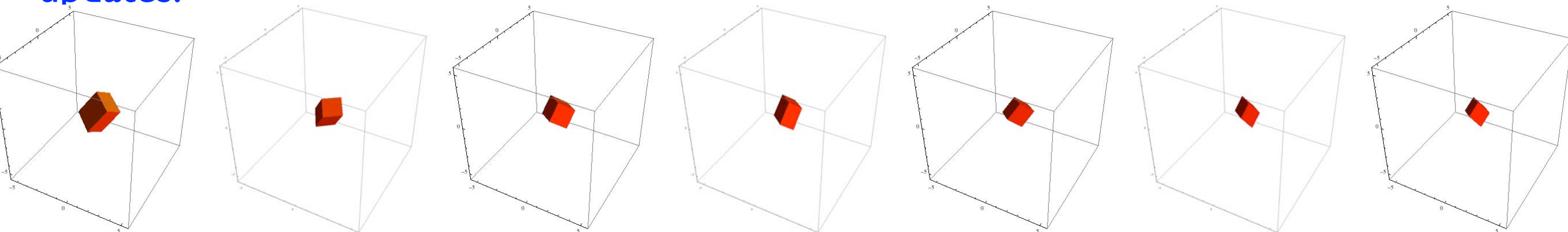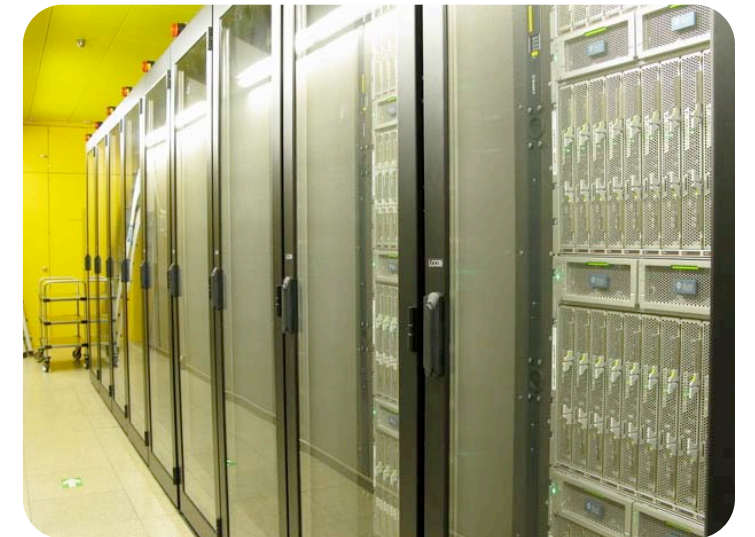
Acknowledgments

A.J. Millis, A. Georges, M. Ferrero, N. Lin, O. Parcollet, P. Werner (2D)
T. Maier, P. Staar, P. Nukala, M. Summers, T. Schulthess (Numerics)
S. Fuchs, L. Pollet, E. Kozik, E. Burovski, T. Pruschke, M. Troyer (3D)

Titane cluster, CEA

Jaguar, ORNL

Brutus cluster, ETH Zurich